Unclassified/Unlimited

SPECTRAL MEASUREMENTS FIELD GUIDE

by

John W. Salisbury

Earth Satellite Corporation

April 23, 1998

Funded by the Defense Intelligence Agency Central Measurement and Signature Intelligence (MASINT) Office (CMO). Sponsored by Paul Lewis, Chairman, SPectroRAdiometric Working Group (SPRAWG).

Published by the Defense Technology Information Center as Report No. ADA362372.

EXECUTIVE SUMMARY

Because of the rapid advance of airborne and satellite sensor technology in providing higher spectral resolution over progressively broader wavelength regions, there is a need for more (and more accurate) field measurements to complement overhead data. The purpose of this field guide is to facilitate such ground-based measurements, first through a review of the environmental factors affecting such measurements, second through an evaluation of the instrumentation involved, and third through a suggested approach to the measurement process.

In evaluating environmental factors affecting spectral measurements in the field, the sources of radiance from a target are discussed in both the reflectance and emittance regions of the spectrum, as well as how those sources are modified by atmospheric attenuation and scattering, and the presence of clouds and wind.

Another factor affecting all spectral measurements in the field is the computer typically used for instrument control and data storage. Computers tend to be the universal weak link in field spectrometers, because of their typical low tolerance for bright sunlight, temperature extremes, windblown dust, and rain. Various solutions to the computer problem are discussed, including the acquisition of hardened computers.

The most commonly used field spectrometers are described, with advice on how to get the most out of each instrument. Then the pros and cons of each instrument are discussed with regard to different applications.

Finally, how to approach field measurements is described, beginning with a thorough testing of a field instrument (and the field instrument user) in the laboratory. Approaches to data collection, record keeping, data reduction, and data analysis are discussed. A major conclusion is that much greater support for data analysis is necessary to reach the full potential of spectroscopic remote sensing for target identification.

TABLE OF CONTENTS

1.0 INTRODUCTION

Most spectroscopic remote sensing applications have been developed in the 0.4 to 14 µm region of the spectrum. It is in this region that electronic transitions and molecular vibration bands offer maximum potential for compositional mapping, and, consequently, this wavelength region is the focus of this report.

Airborne and satellite sensor technology has advanced steadily from broad-band multispectral measurements confined to the visible and near-infrared (VNIR)[1] to progressively more narrow bands extending into the short-wave infrared (SWIR), the mid-wave infrared (MWIR), and long-wave infrared (LWIR). By custom, the wavelength ranges of regions like the MWIR and LWIR are not contiguous but, rather, are bounded by the windows in the atmosphere through which spectral observations of the ground can be made. Thus, although the spectrum itself is continuous, the MWIR and LWIR are generally described as encompassing the 3-5 µm and 8-14 µm spectral regions, respectively.

With advances in sensor technology providing higher spectral resolution data over broader spectral regions, there has been a corresponding need for more (and more accurate) ground-based spectral measurements to complement overhead data. Together, overhead and ground-based measurements will promote the ultimate goal of hyperspectral remote sensing, which is the ability to identify unknown targets in a scene by comparison of their spectral properties with spectra in a search library. The purpose of this field guide is to facilitate ground-based measurements in the 0.4-14 µm region, first through a review of the environmental factors affecting measurement accuracy, second through an evaluation of the instrumentation involved, and third through a suggested approach the measurement process. Below, environmental factors and instrumentation descriptions for reflectance measurements are discussed separately from those for emittance measurements, because of sometimes obvious and sometimes subtle differences that arise between the two wavelength regions.

---

[1] Definitions of terms and acronyms can be found in a glossary in Appendix A.

2.0 BACKGROUND

2.1 Environmental Factors Affecting Reflectance Measurements

2.1.1 Primary Source of Irradiance

Direct illumination by sunlight is the primary source of irradiance for reflectance measurements in the 0.4-2.5 µm (400-2500 nm) region. The intensity of solar irradiance peaks in the visible and declines rapidly into the SWIR. As a consequence, the available signal inevitably declines into the SWIR, which is a generic problem for all passive measurements of reflectance. Field spectrometers typically degrade spectral resolution at longer wavelengths to attempt to compensate for this effect, but a decline in signal-to-noise ratio as 2.5 µm is approached is the norm.

2.1.2 Atmospheric Attenuation

The atmosphere transmits well in the visible, but quite poorly in the infrared. As shown in Figure 2.1a, water vapor has increasingly strong absorption bands from the NIR through the SWIR, with broad regions of complete absorption near 1.36, 1.9 and 2.5 µm. Other atmospheric gases display less strong absorption bands, but some do play a significant role in atmospheric absorption. Ozone absorbs quite strongly at wavelengths shorter than 0.4 µm, and the beginning of this

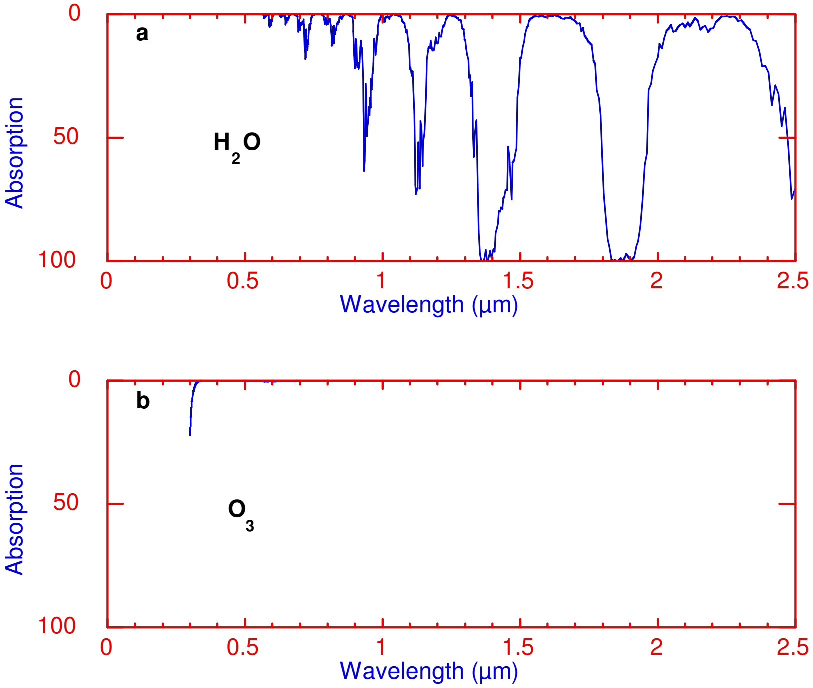
a
H2O
Absorption
0
50
100
0
0.5
1
1.5
2
2.5
Wavelength (µm)
b
O3
Absorption
0
50
100
0
0.5
1
1.5
2
2.5
Wavelength (µm)

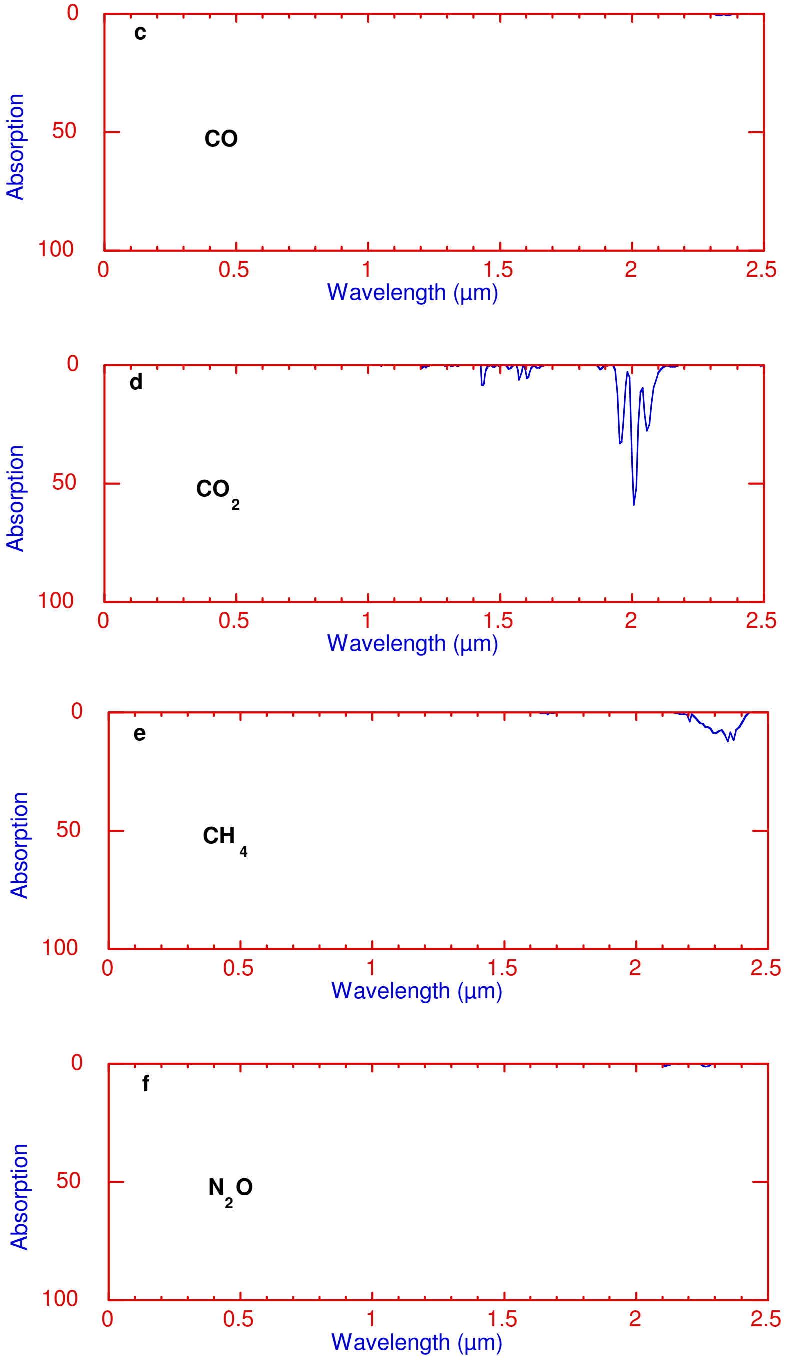
c
CO
d
CO2
e
CH4
f
N2O
Absorption
0
50
100
Wavelength (µm)
0
0.5
1
1.5
2
2.5

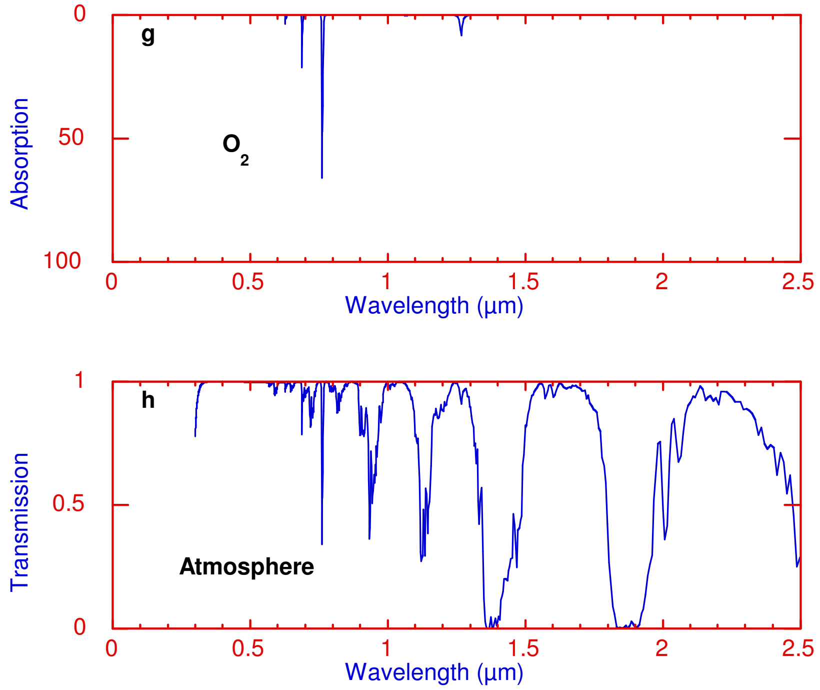

Figure 2.1. Absorption spectra of different atmospheric gases (a-g), and the resulting overall transmission spectrum of a standard atmosphere (h), calculated using the MODTRAN code by Schott (1997).

absorption region is shown in Figure 2.1b, the data for which do not extend to wavelengths shorter than 0.4 µm. Carbon monoxide has a very weak absorption band near 2.33 µm, but carbon dioxide has strong absorption bands near 2.0 µm, and weaker features at shorter wavelengths (Figs. 2.1c and 2.1d). Methane displays a broad absorption region due to a grouping of several absorption bands between 2.2 and 2.4 µm, as shown in Figure 2.1e, while nitrous oxide has very weak absorption bands near 2.22 and 2.36 µm (Fig. 2.1f). Oxygen has some very sharp individual absorption bands, most prominently seen near 0.76 µm (Fig. 2.1g). The overall transmission spectrum of the atmosphere resulting from absorption by all of these gases is shown in Figure 2.1h.

When this atmospheric absorption is superimposed on solar irradiance, the result is very low energy in the SWIR, with broad, highly-absorbing bands centered near 1.36, 1.9 and 2.7 µm. Figure 2.2 illustrates this effect with a spectrum of sunlight reflected from a highly reflecting diffuse standard material, Spectralon®, which is described more fully in Appendix A and Section 5.2.1.

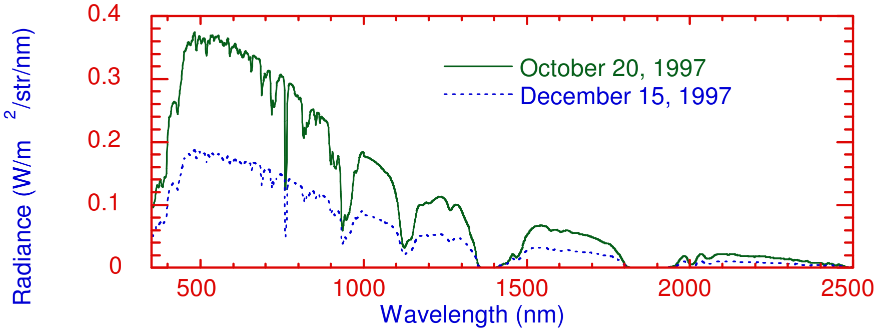

Figure 2.2. Solar radiance after atmospheric attenuation and reflection from Spectralon®. Measurements on clear, sunny days using an ASD FieldSpec® FR by Tim Bowers of Earth Satellite Corp. in Rockville, MD, October 20, 1997, and in Reston, VA, December 15, 1997. The difference in energy would be even greater between December and June measurements.

In view of the importance of absorption by atmospheric water vapor, solar zenith angle becomes a critical measurement parameter, because the column density of water vapor in a given atmosphere increases rapidly as zenith angle increases from its minimum at vertical, either with time of day or with season (see Figure 2.2). Total water vapor content of the atmosphere also tends to vary with season, especially in some geographic locations, so that there is often a trade-off between high zenith angle and total water vapor in the atmospheric column for summertime measurements. All of these aspects of atmospheric water vapor should be considered when planning or executing field measurements.

As water vapor absorption increases, solar irradiance decreases, not just in the middle of absorption bands, but also throughout the SWIR, because the wings of the water vapor bands widen with increasing band strength. This results in lower signal-to-noise for the same integration time, and greater difficulty in detecting spectral features throughout the SWIR, but especially near water band locations. This latter effect is illustrated in Figure 2.3 by the increasing difficulty of detecting the kaolinite doublet absorption bands with increasing zenith angle (compare with laboratory spectra of kaolinite in Figure 3.2a). At a large zenith angle (as at 9 AM, or even 10 AM), the doublet cannot be reliably detected. Just as important, the larger amount of water vapor in the path is accompanied by significant variability from measurement to measurement, introducing distortion of the spectrum in the vicinity of water vapor bands. This variability is illustrated with three consecutive spectra taken about 30 seconds apart, ratioed to the same initial reference spectrum, for each morning time period in Figure 2.3. These measurements represent a best case, at least near sea level, as they were taken under the very low humidity and clear sky conditions typical of a Canadian high pressure system dominating the East Coast of the U. S. in early Fall.

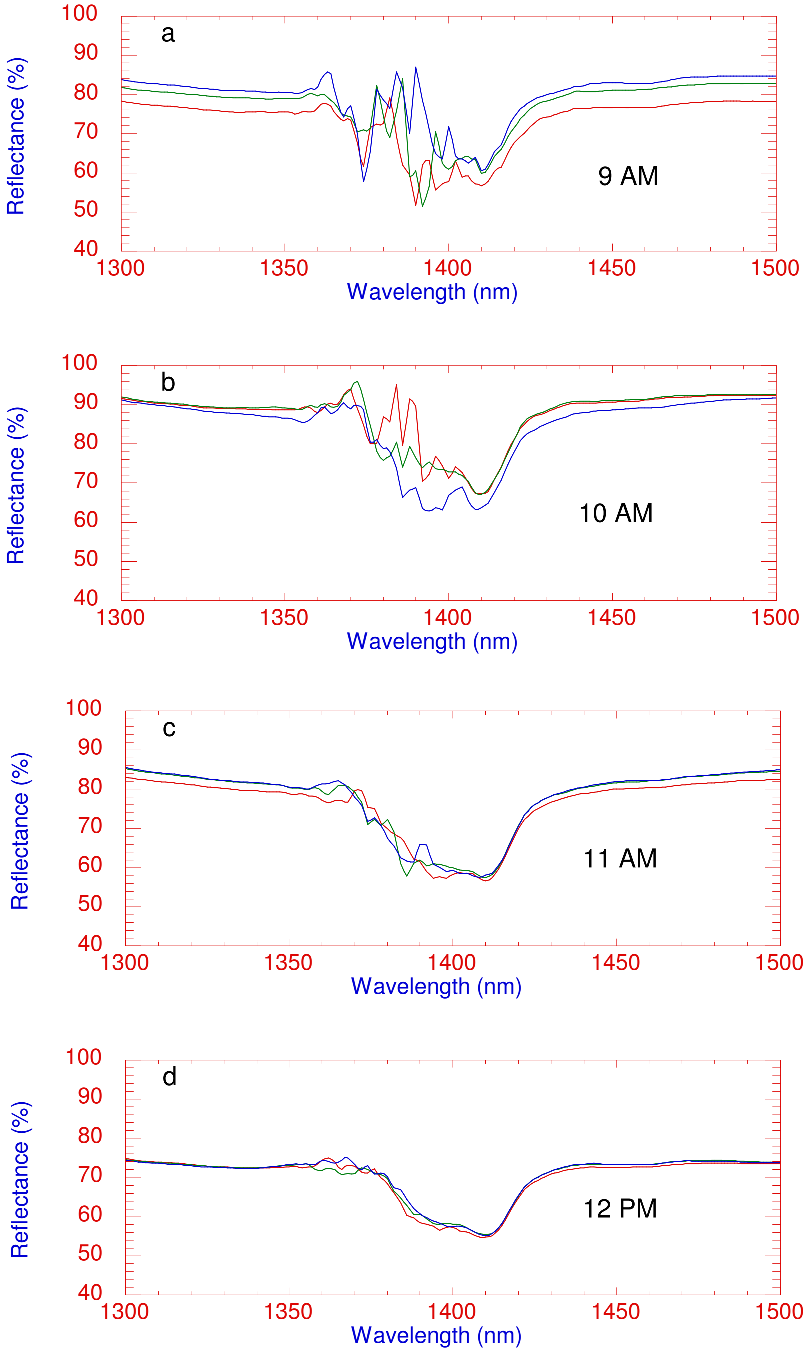

Figure 2.3. Spectral reflectance measurements of kaolinite at four times of day (a, b, c, d), showing the effect of solar zenith angle on the detectability of spectral features in the vicinity of water vapor

bands. Measurements with an ASD FieldSpec® FR by Jim Crowley, U. S. Geological Survey and Tim Bowers of Earth Satellite Corp. in Reston, VA, September 2, 1997. Each spectral curve is the average of 40 scans. Local solar noon would be at about 12:30 PM.

Clearly, when making measurements at low sun angle, one should measure a new reference spectrum for each target measurement.

Superimposed on the large scale changes in water vapor absorption due to zenith angle, season, and geographic location, are smaller variations, both laterally and vertically, that can be very important within a single hyperspectral image. Lateral variations at a kilometer scale have been shown to be significant, even in a desert environment (Green et al., 1991), because water vapor is not a well-mixed atmospheric gas. This same study showed temporal variations of similar magnitude over only 12-minute time intervals. Because water vapor is concentrated at the base of the atmosphere, topographic effects on absorption are also strong (Green, 1991).

The discussion above shows that atmospheric absorption in general, and water vapor absorption in particular, is always going to be a remote sensing problem. It introduces major atmospheric artifacts in the SWIR, such as the spectral gaps caused by complete water vapor absorption (see Figure 2.2), and varies in intensity with time and place, even within a single scene. Thus, upwelling radiance measurements to support calibration/validation of overhead sensors must be made simultaneously with overflight, and strategically placed within the scene (see Section 5.3.1).

Because of spectral artifacts caused primarily by the presence of, and variability of, water vapor (see Figures 2.2 and 2.3), passive field measurements of reflectance are not ideal sources of library spectra to be used in spectral search algorithms for target identification. One solution is to bring samples of target materials into the laboratory for measurement in a controlled environment. However, many materials cannot be brought out of the field because of size, fragility, or simple logistics. Another solution is to use an active measurement of reflectance in the field, which is why we also consider the Pima II in our list of instruments (see section 3.5). Such an active measurement can also be made by using an external radiation source with one of the passive field spectrometers.

2.1.3 Secondary Sources of Radiance

Atmospheric attenuation by absorption is accompanied by scattering, which contributes a significant source of secondary radiance illuminating a target. This "skylight" is spectrally quite different from direct sunlight, being strongly biased toward the blue under clear sky conditions, and lacking appreciable energy in the SWIR, as illustrated in Figure 2.4. On an expanded scale in Figure 2.4. the intensity of skylight can be seen to be about 4% of that of direct sunlight at 1000 nm, 2.5% at 1700 nm, and <1% at 2200 nm.

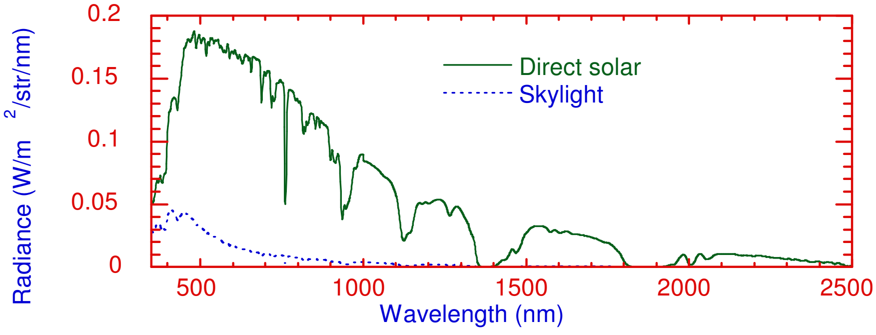

Figure 2.4. Direct solar illumination and skylight reflected from Spectralon®. Measurements with an ASD FieldSpec® FR under clear sky conditions near solar noon by Jim Crowley, U. S. Geological Survey and Tim Bowers of Earth Satellite Corp. in Reston, VA, December 15, 1997. Each spectrum is the average of 40 scans.

Under clear sky conditions, total skylight is only about 8% as strong as direct sunlight when the sun is near the zenith, but is about 60% as strong as direct sunlight when the sun is near the horizon (Fenn et al., 1985). This increases the blue component of target illumination but, more important, the SWIR component is reduced, along with the signal to noise in this region of the spectrum. In the extreme case, when a target is in shadow, it is only illuminated by skylight. Thus, spectral features in the SWIR are simply not available for target detection or identification.

Scattering by aerosols will increase skylight, and the higher the concentration, the greater the skylight intensity. In addition, larger aerosols scatter more uniformly in the visible, and further out into the infrared. Thus, under a very hazy sky, total skylight may vary from about 13% of direct sunlight with the sun at zenith, to equal in intensity when the sun is near the horizon (Fenn et al., 1985). Even with large aerosols, however, skylight intensity in the SWIR is very low, because of the lack of scattering by even large aerosols at these longer wavelengths.

Another source of secondary illumination is so-called "background radiance", which arises from sunlight reflected from, or transmitted through, background materials (see Figure 2.5). The spectral character of sunlight is modified by the reflectance or transmittance spectrum of the background materials, thus affecting the apparent spectral signature of the target. This is usually not a significant source of error, except when the background object is large enough or close enough to subtend a large portion of the solid angle viewed by the target (see

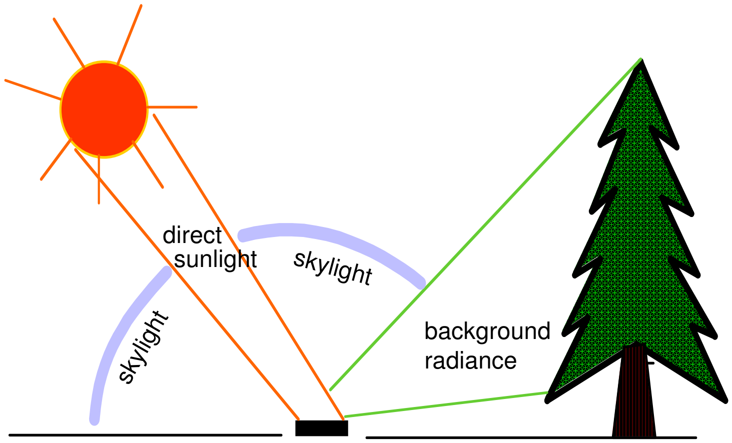

Figure 2.5. Sources of radiance onto a target. (Modified from an illustration on an Analytical Spectral Devices Web site: http://www.asdi.com/apps/remote_sensing.html).

Figure 3.1 and text of caption). Thus, the magnitude of background radiance compared to direct solar illumination and skylight is typically small, except in special situations. One such situation pointed out by Schott (1997, p. 49) is when the target is a specular material and the background source is bright and viewed at the specular angle.

Another special situation is common enough to be of concern, which is when a target is otherwise visible to an overhead sensor, but is in the shade of a tree canopy. Sunlight filtered through green leaves with their high water content has a greatly reduced SWIR component, especially in the 1.4-2.5 µm region surrounded by water bands. Thus, a target illuminated principally by skylight and background radiance transmitted through the canopy typically may reflect detectable energy only in the visible through the shortest wavelength region of the SWIR (i.e., out to ~1800 nm). Again, this distortion of target signature can make detection or identification difficult or impossible, depending on the wavelengths of the identifying spectral features.

2.1.4 Clouds

Clouds attenuate solar irradiance, and thus inevitably degrade signal-to-noise, especially in the SWIR. Because of the ability of our eyes to accommodate different visible light levels, the importance of this effect is often underestimated. Figure 2.6 illustrates this point with radiance spectra of direct sunlight and skylight reflected from a highly reflecting diffuse standard under both clear sky and hazy sky conditions. The hazy sky illumination resulted in distinct shadows, but with diffuse edges, and might be described visually as "cloudy bright". In addition to reducing the energy available for measurement, the hazy sky resulted in highly variable irradiance. This is illustrated in Figures 2.7a and 2.7b, which show reflectance spectra of kaolinite taken under clear and hazy conditions, respectively. In each case, a single reference spectrum was taken, followed by a series of reflectance measurements, with Figures 2.7a and 2.7b showing the

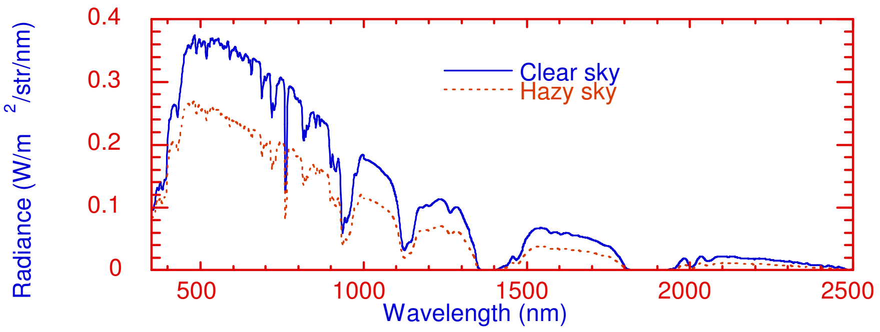

Figure 2.6. Solar radiance under clear and hazy skies after reflection from Spectralon®. Measurements in Rockville, MD by Tim Bowers of Earth Satellite Corp., using an ASD FieldSpec® FR, on October 20, 1997 (clear sky) and October 16, 1997 (hazy sky).

apparent variability of reflectance caused by variations in irradiance after the time the reference panel was measured. This again demonstrates the importance of re-measuring the reference panel often (preferably immediately before or after each target measurement) when atmospheric conditions are less than perfect.

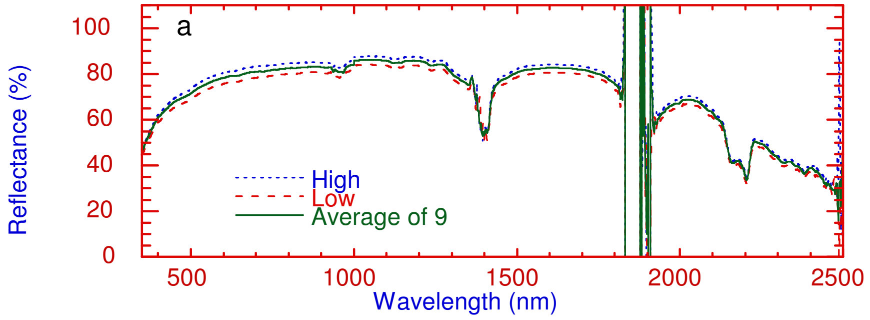

Figure 2.7a. Average reflectance of nine consecutive measurements of kaolinite following a single reference measurement, as well as the highest and lowest apparent reflectance caused by changes in atmospheric absorption and solar irradiance after measurement of the reference. Clear sky measurement with an ASD FieldSpec® FR by Tim Bowers of Earth Satellite Corp. in Rockville, MD, October 20, 1997.

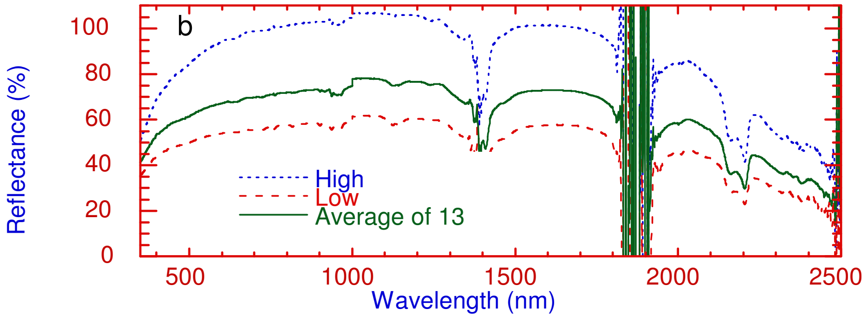

Figure 2.7b. Average reflectance of thirteen consecutive measurements of kaolinite following a single reference measurement, as well as the highest and lowest apparent reflectance caused by changes in atmospheric absorption and solar irradiance after measurement of the reference. Cloudy sky measurement with an ASD FieldSpec® FR by Tim Bowers of Earth Satellite Corp. in Rockville, MD, October 16, 1997.

2.1.5 Wind

Wind is a minor variable for most reflectance and radiance measurements, except for targets that are physically affected by wind. The leaves of a vegetation canopy, for example, are twisted by the wind, exposing their undersides which can have a different spectral signature than the upper surfaces. This also tends to change the canopy geometry, and thus the ratio of leaf surface exposed compared to shade, and compared to the ground surface seen through the canopy. Under windy conditions, it is recommended that many spectra of such targets be averaged to reduce the effects of these variables.

The largest difference caused by wind is in the reflectance of an otherwise still water body. The more diffuse bidirectional reflectance distribution function (BRDF) of a water surface rendered choppy by wind results in glitter, which is much brighter than the reflectance from a flat surface of calm water, when measured away from the specular angle.

2.2 Environmental Factors Affecting Emittance Measurements

2.2.1 Primary Source of Radiance

Solar irradiance declines rapidly from its peak in the visible toward zero near 3 µm, after attenuation by atmospheric absorption (see Figure 2.2). At the same time, thermal emission by surface materials at room temperature decreases in the other direction from peak radiance near 9.6 µm to near zero at 3.0 µm (see

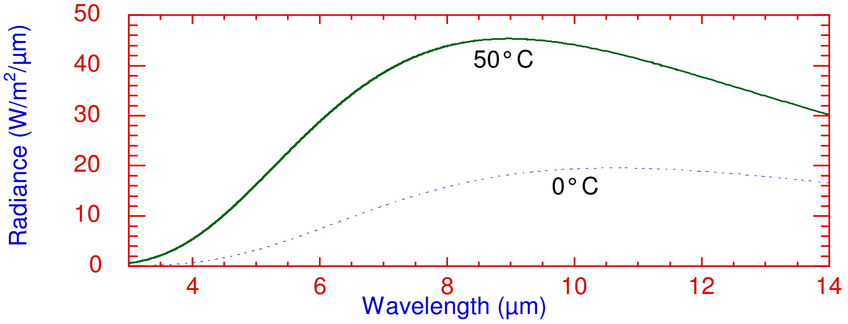

Figure 2.8. Radiance from 50° C and 0° C blackbodies (calculations courtesy of Andrew Korb, SAIC).

Figure 2.8). Much is often made of the confusion posed by the crossover point (point at which the intensities of reflected and emitted energy are equal) for remote sensing measurements in the 3-5 µm atmospheric window. For room temperature targets, this is typically between 3.0 and 3.5 µm, depending on sky clarity, solar zenith angle, and the reflectance and temperature of the surface. In fact, the very low energy from either source in that wavelength range (compare Figures 2.2 and 2.8), coupled with atmospheric absorption, prevents meaningful remote sensing measurements in the usual crossover region. In the narrow window region between 3.5 µm and the beginning of strong CO_2 absorption at 4.2 µm (see next section), reflected sunlight can be a significant fraction of detected radiance under certain conditions, the most common of which is for a smooth surface viewed at the specular angle with the sun. Many manmade materials have smooth surfaces with a substantial specular component to their reflection, and manmade objects often have complex geometry. Thus, some facet of the object can be at the specular angle with the sun, and thus provide a "hot spot" of radiance containing a significant solar component. This would be especially true of smooth bare metal surfaces, which have high reflectances (and, hence, low emissivities) in the 3-5 µm region. Another obvious condition under which solar reflectance may be a significant fraction of detected radiance is in relatively cold environments (see Figure 2.8). A rare condition that could contribute a significant solar component would involve a highly reflecting diffuse surface with a correspondingly low emissivity. Most materials have a low reflectance in this wavelength region, including materials like snow, which has a very high reflectance in the visible but a very low reflectance in the 3-5 µm region. Metals are one exception to this rule, and a rough metal surface would satisfy this rare condition. Even in these special cases, when reflected solar energy is a significant fraction of radiance in the shorter wavelength portion of the 3-5 µm window, reflected solar energy is still negligible beyond the CO_2 absorption range (4.2 µm-4.4 µm).

For smooth surfaces viewed at other than the specular angle with the sun, or for diffuse surfaces with low reflectance and hence high emissivity (typical for most materials), or for relatively warm surfaces, self-emission strongly dominates detected radiance throughout the usable portion of the 3-5 μm atmospheric window. Thus, the primary source of radiance in both the MWIR and LWIR is self-emission by the target material. The energy available for remote sensing measurements is much greater in the LWIR, as shown in Figure 2.8.

2.2.2 Atmospheric Attenuation

As illustrated in Figure 2.9, absorption by atmospheric gases in the wavelength region of thermal emittance can be severe. The figure illustrates absorption by a standard atmosphere, but note that bands displaying 100% absorption are sufficiently strong that the atmosphere completely absorbs self-emission from a target, even over a distance as little as the one meter typical of a field measurement. The chief absorber is water vapor, the absorption of which

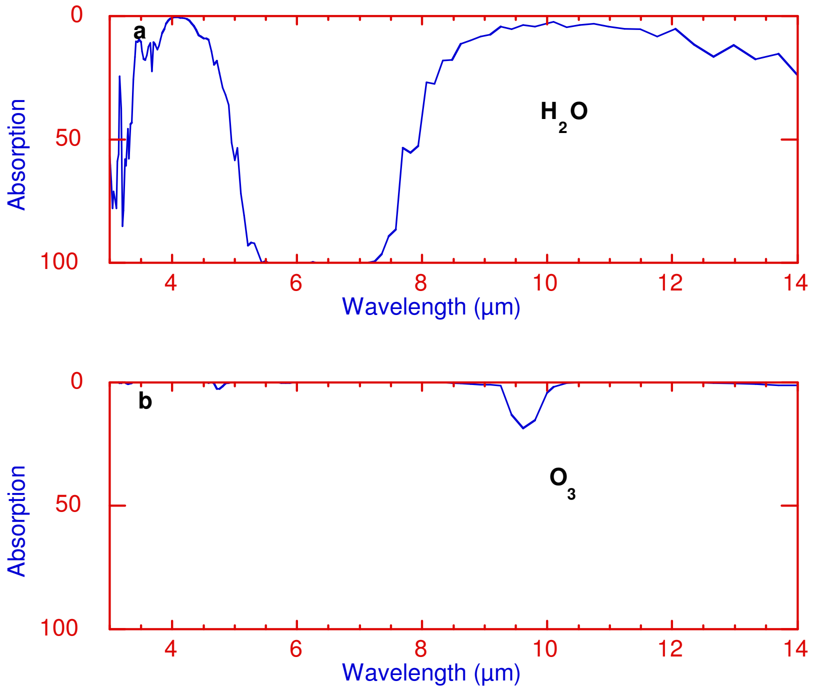

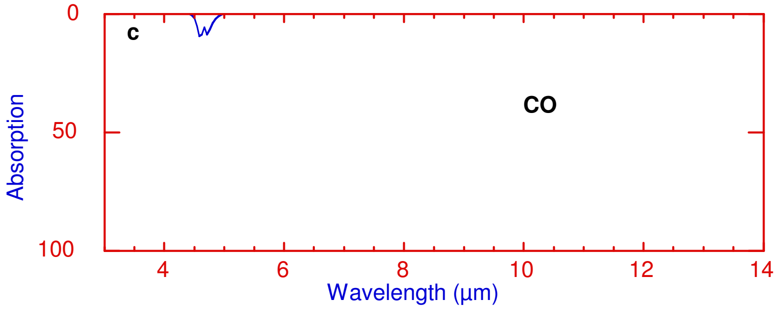
c
CO
Absorption
0
50
100
4
6
8
10
12
14
Wavelength (µm)

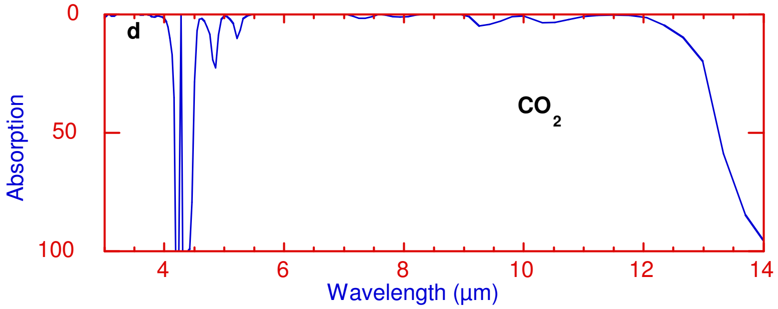
d
CO2
Absorption
0
50
100
4
6
8
10
12
14
Wavelength (µm)

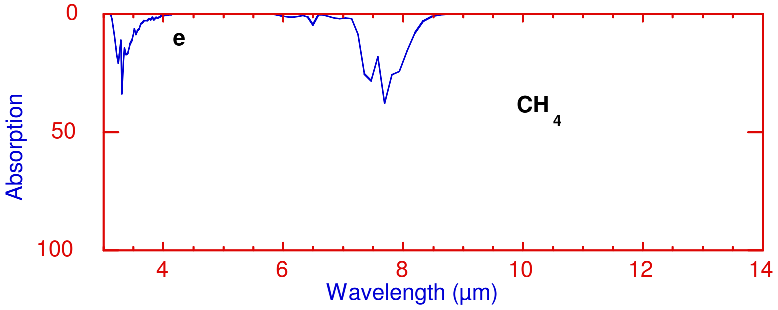
e
CH4
Absorption
0
50
100
4
6
8
10
12
14
Wavelength (µm)

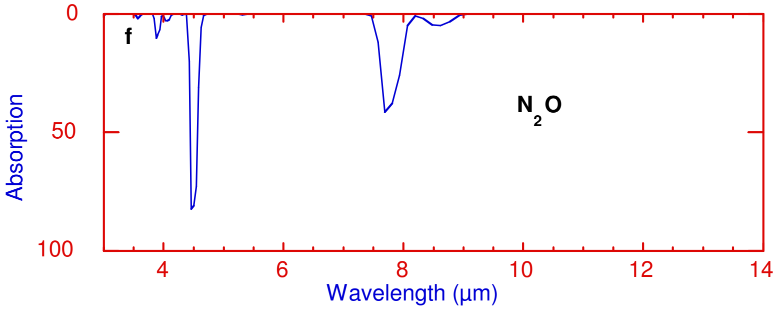
f
N2O
Absorption
0
50
100
4
6
8
10
12
14
Wavelength (µm)

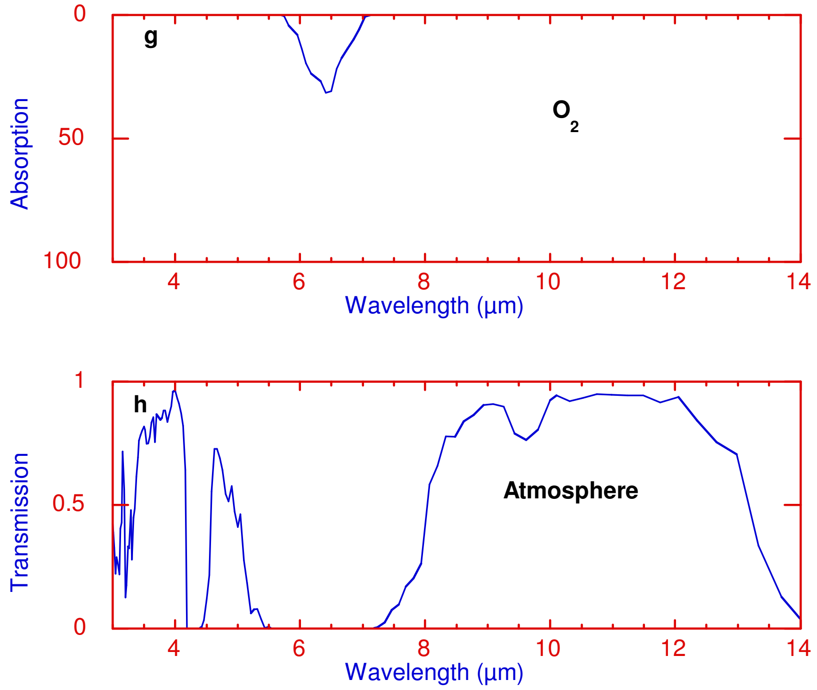

Figure 2.9. Absorption spectra of different atmospheric gases (a-g), and the resulting overall transmission spectrum of a standard atmosphere (h), calculated using the MODTRAN code by Schott (1997).

defines both sides of the 3-5 µm window, and the short wavelength margin of the 8-14 µm window. Carbon dioxide is the next most important absorber, introducing very strong absorption bands between 4.2 and 4.4 µm, and defining the long wavelength side of the 8-14 µm window. Other gases of importance are nitrous oxide, which contributes a strong band near 4.5 µm that extends the gap in the 3-5 µm window caused by CO_2; and methane, which contributes to the absorption of water vapor between 3.0 and 3.5 µm.

One significant result of all of these absorption bands is that the 3-5 µm window does not fully "open" until 3.5 µm, and has an absorption gap between 4.2 and 4.5 µm, leaving little room for spectral remote sensing. This lack of spectral breadth, taken together with the low energy available in this region (except for hot targets), makes the 3-5 µm window typically less favorable for spectral remote sensing than the 8-14 µm region.

2.2.3 Secondary Sources of Radiance

As in the reflective region of the spectrum, secondary radiance arises in both the atmosphere and from background objects in the field of view of the target. In the emittance region, however, the atmosphere and background materials are themselves emitting the radiation.

Atmospheric gases emit primarily in the same narrow bands where they absorb (see downwelling radiance spectrum in Figure 2.10), although there is also what is called "continuum" emission in regions that are otherwise atmospheric windows, comprised of the distant wings of all bands. Large aerosols (see section on clouds below) and background materials, on the other hand, emit more like blackbodies. Atmospheric radiance is usually not distinguished from radiance arising from background objects, as it is in the reflective region (e.g., skylight vs. background radiance). Instead all sources are usually lumped together as "background radiance," or "downwelling radiance," which is reflected from the target. One of the important efforts in field measurements is to distinguish between self-emission of the target and the downwelling radiance reflected from it (see Sections 5.3.2 and 5.5.2). Only by separating the two can the emittance of the target be determined and the emissivity calculated.

The importance of downwelling atmospheric radiance is illustrated in Figure 2.10, where the two upper curves represent spectra of the radiance (self-emission plus reflected downwelling radiance) measured from a quartz sand, and the lowest curve represents atmospheric downwelling radiance (DWR) reflected from a highly reflecting diffuse surface. The primarily atmospheric origin of the downwelling radiance is indicated by the many sharp water vapor emission lines, particularly between 8.0 and 9.0 µm, as well as the broad ozone emission doublet between 9.2 and 10.0 µm. (Note that these water vapor lines are not apparent in Figure 2.9a because that figure was generated with low resolution data.)

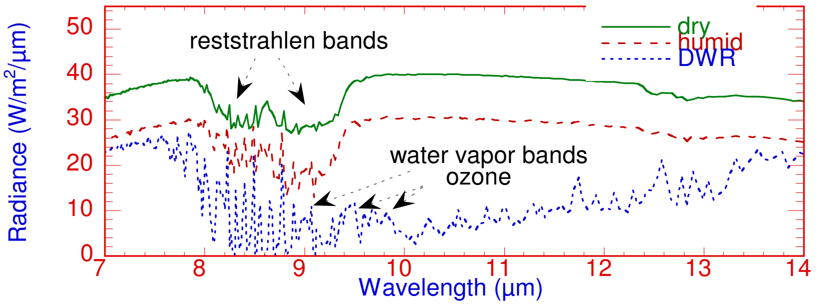

Figure 2.10. The two uppermost curves are radiance spectra of quartz sand measured in dry desert and humid subtropical environments. The lower curve is a downwelling radiance (DWR) spectrum associated with the humid environment. Measurements were made with the microFTIR spectrometer. The upper quartz

radiance spectrum has been offset upward by 10 units for clarity (from Korb et al., 1996).

The water vapor emission lines in the downwelling radiance are strongly reflected in the fundamental molecular vibration bands (reststrahlen bands) in the quartz radiance, which form two broad minima between 8.0 and 9.5 µm. These water vapor lines are preferentially reflected in the reststrahlen bands because these emittance minima are reflectance maxima, in accordance with Kirchhoff's Law (E=1-R). Where quartz does not reflect strongly, the atmospheric emission bands are much less obvious in the radiance spectrum. Thus, what the upper two spectral radiance curves show in Figure 2.10 is that atmospheric downwelling radiance can be a very significant fraction of radiance due to target self-emission (and virtually equal at either edge of the atmospheric window), but that this atmospheric component varies with atmospheric water vapor content, and with the wavelength-dependent reflectance of the target material.

Not only does a dry environment reduce atmospheric downwelling radiance, the principal source of which is water vapor, but also the downwelling radiance tends to be much more stable with time. This stability is an important factor in the accuracy with which the emissivity of a target material can be derived, because all current thermal infrared field spectrometers are single-beam instruments. Thus, target radiance and downwelling radiance must be measured sequentially. In a humid environment, downwelling radiance may change faster than sequential measurements can be made, introducing a significant source of error in accounting for its effect in deriving target emissivity (Korb et al., 1996; and see Section 5.3.2).

Another source of downwelling radiance is any warm object in the field of view of the target. This effect is often overestimated, as when investigators move their field spectrometer far back from the target to reduce the solid angle intercepted by this relatively warm object. However, calculations show that even the relatively large Bomem spectrometer (see Section 4.2.1) obscures only about 5% of the field of view of a target at a distance of one meter. The side of a nearby truck heated by the sun, on the other hand, could be a significant source because of both relative size and temperature. Backing the field spectrometer off many meters from the target, however, can introduce atmospheric absorption and scattering problems that far exceed those represented by downwelling radiance, which can be measured and subtracted from target self-emission (see Section 5.5.2).

2.2.4 Clouds

Clouds can be a very potent source of downwelling radiance, especially when low in the atmosphere, and hence relatively warm. Scattered clouds, such as cumulus, are typically a highly variable source of radiance as they move across the sky (and across the field of view of the target). A more uniform layer of cloud, such as stratus, provides more constant downwelling radiance. One important aspect of cloud radiance compared to atmospheric gas radiance is its spectral character. That is, clouds radiate essentially as blackbodies, instead of having the sharp band structure of gas emission, as illustrated in Figure 2.11.

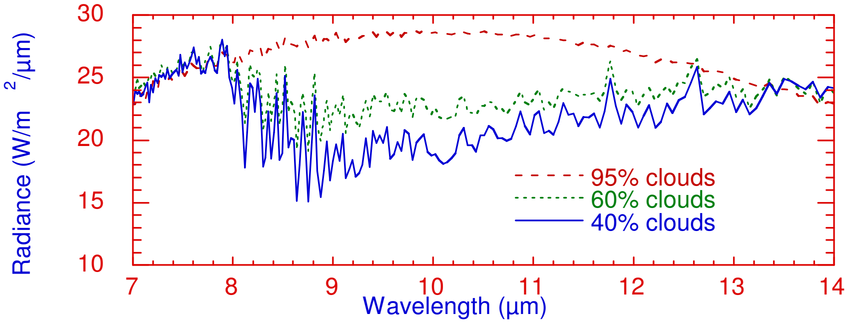

Figure 2.11. Changing downwelling radiance with changing percentage of cloud cover measured with a GER Thermal IRIS spectrometer (from Salisbury, 1990).

2.2.5 Wind

Determining the temperature of the target is a critical part of deriving emissivity, and a temperature that changes during measurement because of intermittent wind cooling will introduce error. This is a significant problem with low thermal inertia materials like soils, and materials like water (or damp soil) that undergo rapid evaporative cooling in the very near-surface layer from which infrared radiation is emitted (the infrared skin depth).

Wind can also be a source of error in measurement of downwellling radiance. Although downwelling radiance can be measured directly with a series of upward-looking measurements, it is more often determined by measuring the radiance reflected from a substantially diffuse, highly reflecting surface (see Section 5.3.2). It is necessary to determine the temperature of this reflective material, at least during field measurements. The temperature of this material must be known to distinguish between reflected downwelling radiance and self-emission by the reflector. The very low emissivity of materials typically used to reflect downwelling radiance, such as a diffuse gold plate or crinkled aluminum foil, makes this a relatively small error, although it can become significant when these materials are heated to high temperature by exposure to the desert sun. Crinkled aluminum foil taped to cardboard is often used for field measurements of downwelling radiance because it is light, can be manufactured to any desired size, and can be easily renewed after contamination by windblown dust. However, it has such low thermal mass that its temperature fluctuates rapidly as a result of intermittent wind cooling. On the other hand, continuous wind cooling can be useful in determining the temperature of a foil surface, since it very rapidly converges with air temperature under the influence of wind.

2.3 Other Factors Affecting Measurements

2.3.1 Computers - The Universal Weak Link

All modern field spectrometers are computer-controlled, but most computers were not designed for field use. Thus, the typical laptop computer has several generic problems that should make the user wary, and specifications should be carefully written during purchase of a field spectrometer to meet anticipated applications. Problems to consider are discussed below, followed by suggested solutions.

Screen Visibility. It is very difficult to purchase a laptop computer with anything but a color screen. However, the typical color screen is virtually invisible in bright daylight. One solution is to buy a computer with a brighter color screen that can more or less compete with daylight, but this requires more electrical power, and hence additional battery weight for the same time of operation (more irritating than the extra weight is the necessity to change batteries repeatedly, as often as every half hour for some computers). The best solution is to find a monochrome screen, as long as the field instrument control program does not depend on color cues. A reflective monochrome screen is most visible in bright daylight, and uses the least power, except when it needs a backlight to be visible in the dark or indoors. A transflective monochrome screen is a good compromise that is visible both indoors and out, but it is not as visible in daylight as a completely reflective screen.

Temperature Tolerance. Room temperature is not the norm for field measurements, but most computers are built to operate at room temperature. The typical LCD screen, for example, fades out at temperatures below about 3.5° C (38°F) and above about 33.5° C (92°F). CPU's also have a limited temperature operating range, although usually significantly greater than the screen. Thus, when a vendor quotes an operating range, it should be determined whether or not this range includes screen visibility.

The author has seen several rough-and-ready solutions to temperature intolerance, such as keeping the computer under one's shirt between measurements in cold weather, wrapping the computer in a sweatshirt which has been periodically soaked with liquid nitrogen in hot weather, and simply taping aluminum foil to the outside of the lid to reflect sunlight. A more sophisticated solution, such as a climate-controlled carrying case, tends to be heavy and a serious power drain. Most desirable of all is a temperature-tolerant computer that requires no special care.

Dust and Rain Tolerance. Windblown dust is a common problem in the desert, and both keyboards and floppy drives can be totally disabled by dust contamination. Sudden rain storms can occur in any environment, and the typical laptop does not tolerate getting wet. Some degree of hardening is desirable, and a sealed keyboard is probably the most important hardening step to take. An ordinary keyboard can be covered with plastic wrap as a stopgap measure.

Weight and Power. The initial weight of the computer itself is compounded by the added weight of enough batteries to keep it working for the desired length of time. The direction of the portable spectrometer industry with regard to computers varies with vendor. Designs and Prototypes is working on an instrument that will have a computer board integrated with the electronics in a temperature-controlled environment, with a minimal external controller (a smart instrument, rather than a dumb instrument and a smart computer). Analytical Spectral Devices is reportedly adopting a Windows-capable, 2-lb palmtop Toshiba to replace its sub-notebook controller. Geophysical and Environmental Research appears more concerned with screen visibility and temperature, dust, and rain tolerance than with size. They are currently working with the Rocky series of laptop computers from Amrel Systems, Inc., which are hardened to withstand both weather and temperature extremes. Amrel is also one of the few companies offering a laptop with a transflective monochrome screen, as well as daylight-visible color. Users who are interested in such a computer can visit the Amrel Web site (www.amrel.com) or call Tom Corl of GER for further information (914-677-6100).

Another rugged computer that has been used in the field with some success is the Husky, produced by Husky Computers, Ltd. of Coventry, England. The British Natural Environment Research Council maintains a centralized equipment pool for field spectroscopy at the University of Southampton. Dr. Charles Kerr, on the equipment pool staff, reports that the Husky model Px5 solves many of the problems that they have experienced with ordinary laptop computers. It is weather and temperature tolerant, and also has a transflective monochrome screen for daylight visibility. Users who are interested in the Husky can visit the Husky Web site (www.wpihusky.com), or correspond with Dr. Kerr (epfs@soton.ac.uk) for further information.

3.0 INSTRUMENTS OF THE REFLECTIVE REGION

3.1 General

There are many field instruments that operate in the VNIR, but we review here only the most widely used instruments that operate into the SWIR (and, in the case of the Pima II, an instrument that operates only in the SWIR). The reason for this approach is that the SWIR is the most important wavelength region for compositionally diagnostic spectral information. The electronic transition bands found in the visible lend color to objects, but color has limited usefulness, since different objects with the same composition can be any color. Molecular vibration bands, on the other hand, are typically more representative of the bulk composition of the material. While the fundamental molecular vibration bands of most materials occur in the MWIR and LWIR, overtones and combination tones of these features often occur in the SWIR, both in the 1.5-1.9 µm region and (more abundantly) in the 2-2.5 µm region. These regions of the spectrum thus become highly important for many remote sensing applications.

The reader should recognize that any review of field spectrometers is a snapshot of a moving target. Innovations and improvements occur to meet market requirements, and most of the manufacturers can, and sometimes do, produce custom instruments that overcome limitations of their standard products pointed out below. Thus, these descriptions and tips should be taken as a guide for further inquiry, rather than the last word on the subject.

In this discussion of field spectrometers, reference is made to spectral resolution, an important instrument attribute for most applications. Any discussion of spectral resolution is complicated by the fact that it is defined differently by different people. For the reader to understand the terms used in this report, a brief explanation is offered here using the classic grating spectrometer as an illustration. A grating disperses the spectrum for measurement of the relative intensities of different wavelengths. Rotation of the grating scans the dispersed spectrum past a slit, which isolates intervals of the spectrum for individual measurement by a detector. The width of the slit defines the spectral sampling interval (the same role essentially played by individual detectors in a detector array). Data may be recorded or resampled at wavelength intervals shorter than the sampling interval, but this serves only to smooth the curve by interpolation, rather than to generate higher spectral resolution. If the spectrometer observes a monochromatic source of radiation, a Gaussian curve of detector output results as this source passes across the slit, and the poorer the resolution, the broader the curve. The width of this Gaussian curve at half its height (full width at half maximum, or FWHM) is a commonly accepted definition of the resolution of an instrument. In this report, spectra of the same materials measured by different instruments are shown, so that readers can draw their own conclusions about resolution.

3.2 ASD FieldSpec® FR By Analytical Spectral Devices, Inc.

3.2.1 Instrument Description

The ASD FieldSpec® FR spectroradiometer combines three spectrometers to cover the wavelength range from 350 to 2500 nm. A photodiode array spectrometer is used to cover the 350 to 1000 nm spectral range (UV/VNIR), while two fast-scanning (0.1 sec) spectrometers provide coverage for the two wavelength ranges from 1001 to 1800 nm and 1801 to 2500 nm (SWIR 1 and SWIR 2). The UV/VNIR range uses a 512-element photodiode array operated at ambient temperature with a fixed grating as dispersive element. Single-element, thermoelectrically-cooled InGaAs detectors are used in the two SWIR spectrometers, with moving gratings that rapidly scan the spectrum across the detectors. Although a 0.1 sec scan is available, which can be useful when monitoring rapidly changing targets, for most applications the scan-averaging mode is used to increase signal-to-noise. Most targets provide excellent (1000/1 or better) signal-to-noise when 40 scans are averaged in four seconds, but about a minute is required for initial optimization of gain settings and correction for dark current, an operation which should be repeated when observing conditions change. The time for this operation has to factored into overall measurement time, but usually many spectra are measured between optimizations.

Figure 3.1. Jim Crowley, U. S. Geological Survey, points the ASD FieldSpec® FR fiber optic cable at a Spectralon® reference panel.

> (For purpose of illustration, Dr. Crowley is standing in full sun quite close to the panel. His illuminated pants leg and shirt in such a configuration would present a significant source of background radiance better minimized. This could be done by standing further away and/or on the other side of the reference panel, so that his illuminated side faced away from it. Dark clothing is also a plus. In the event that such a source of background radiance cannot be avoided, the important thing is to keep it constant for measurement of both reference and target.)

Radiation input to the ASD FieldSpec® FR spectrometers is through a fiber optic bundle, nominally 1.2 meters in length[1]. The fiber optic cable is typically fed through a pistol grip for easy pointing (see Figure 3.1), but more precise aiming optics (both laser spot and telescopic sight types) are available as options. The optical fibers carrying radiation to the spectrometers are packaged as a single bundle exterior to the instrument. Once inside the instrument, the fibers are separated into three bundles which then deliver the collected radiation to each of the three spectrometers. The common probe end has a nominal 25° field of view, with optional foreoptics that include a cosine receptor for irradiance measurements, and foreoptics that restrict the field of view to 8° or 1°. The instrument is controlled, data displayed in real time, and stored using a sub-notebook computer integral to the instrument. The computer is usually powered by its own battery, but both computer and spectrometer can be powered by rechargeable NiCad batteries that are worn in a fanny pack (2.2 kg), while the computer and spectrometer (7 kg) are suspended in front from a shoulder harness (see Figure 3.1).

Spectral resolution in the visible is not a problem for any of these field instruments because of the greater energy available and the relatively high detector sensitivity. In the more troublesome SWIR, how well the different instruments perform is illustrated in this report by how well each will resolve the narrowest bands likely to be sought for different applications in the two SWIR regions on either side of the 1.9 µm water absorption band.

Figure 3.2a shows that the ASD FieldSpec® FR distinctly, but incompletely, resolves the kaolinite doublet with minima 20 nm apart in the shorter wavelength, SWIR 1, region. The incompleteness of the band resolution appears to the author to indicate a spectral resolution for the instrument of between 10 and 15 nm, but this is sufficiently a judgment call (because the absorption bands are not line sources of equal intensity, or even Gaussian, but rather an asymmetric triplet) that he does not argue with the manufacturer's claimed 10 nm resolution. More Gaussian absorption bands 25 nm apart in the SWIR 2 region in Figure 3.2b, on the other hand, are completely resolved, which is certainly consistent with 10 nm resolution in this region. Note that this particular ASD FieldSpec®

---

[1] While longer fiber optic cables can be used, absorption in the optical fibers becomes a problem. With the 10-m cable option provided by ASD, spectra begin to deteriorate at 2200 nm, and become very noisy by 2400 nm..

FR instrument does show a slight (4 nm) wavelength offset to shorter wavelength. This magnitude of wavelength error is common in scanning instruments after being subjected to the rigors of field use, and illustrates the necessity for periodic checking of instrument performance, including wavelength calibration.

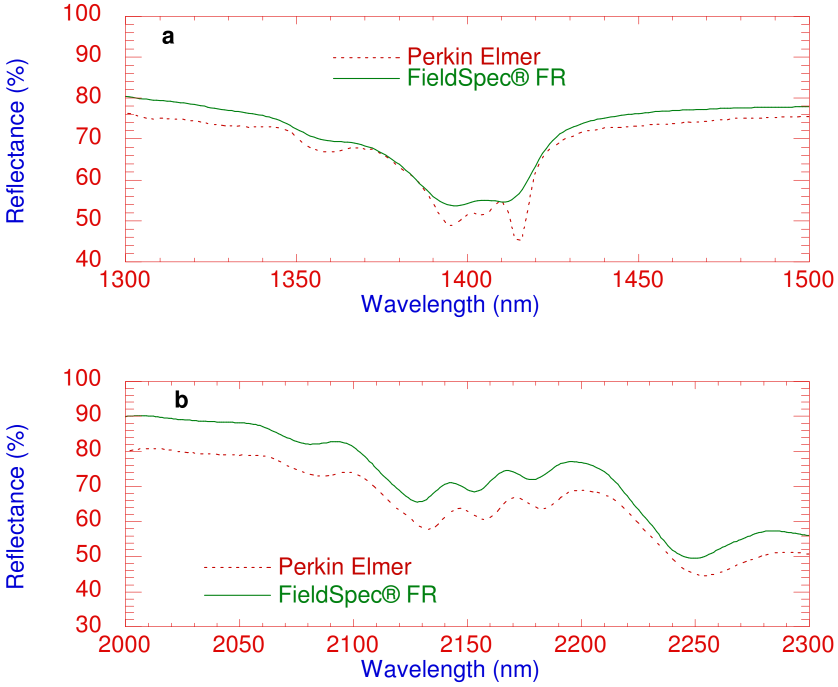

Figure 3.2. (a) shows a laboratory directional hemispherical reflectance spectrum of kaolinite measured by a Perkin Elmer Lambda 900 spectrometer compared to a bidirectional spectrum of the same sample measured by the ASD FieldSpec® FR. The kaolinite absorption band minima on either side of 1400 nm are 20 nm apart. (b) shows a similar comparison of the spectrum of polyester fabric. The three highly distinctive absorption bands between 2100 and 2200 nm are about 25 nm apart. Bidirectional measurements are not expected to yield the same absolute reflectance values as directional hemispherical measurements, because of the difference in geometry. (All spectra measured by Jim Crowley, U. S. Geological Survey).

Table 1. ASD FieldSpec® FR manufacturer's specifications as of December, 1997 (comments in parentheses are the author's).

Spectral Range	350-2500 nm

Spectral Sampling	1.4 nm over the range 350-1000 nm 2 nm over the range 1000-2500 nm
Data Interval	Data resampled to 1 nm intervals
Spectral Resolution	3 nm over the range 350-1000 nm 10 nm over the range 1000-2500 nm (However, see Fig. 3.2 and text discussion)
Field of View	25° nominal with 1°, 8°, and 2 pi optional
Scan Time	0.1 sec (40 scans usually averaged to achieve good S/N, which takes 4 sec, plus prorated time for periodic 60 sec optimization. The spectra in Figure 3.2 were measured with 40 scans)
Power Source	External NiCad rechargeable batteries
Size	35 x 29 x 13 cm
Measurement type	Single beam bidirectional, requiring either a solar or artificial external light source.
Weight	7 kg plus 2.2 kg battery pack (this is the nominal operational weight of the spectrometer with pistol grip aiming device, without better aiming optics or lightweight tripod, both of which are recommended for highest quality data. These items would add ~3 kg. Necessary items that can be left in a car, such as spare batteries, battery charger, etc. are extra).

3.2.2 Instrument Tips and Rules of Thumb

Sensitivity Drift. ASD FieldSpec® FR sensitivity changes with temperature, and this is particularly significant when it is warming up. The manufacturer and all users recommend an extended warm-up period of from one to two hours to improve instrument stability and the repeatability of measurements, especially of radiance, but also of reflectance. In view of limited battery life, this warm-up period can most conveniently be accomplished in an automobile using the cigarette lighter attachment for power. It is not clear that sensitivity drift ever stops, particularly when the instrument is subject to heating or cooling stress under field conditions. In fact, were the instrument designed primarily for radiometry, one would expect all of the detector modules to be temperature-controlled (such a custom configuration is available from ASD for additional cost).

Terry Hemmer of SITAC, in cooperation with Mark Czarnaski and William Graver of the Naval Research Laboratory, measured sensitivity drift by making radiance measurements of a constant source for two hours in a laboratory environment. The measurements were made during instrument warm-up, but were not started until several minutes after the spectrometer was turned on. Dark current corrections were not made during the radiance measurements, although they would be part of normal operating procedure, because the objective was to determine uncorrected instrument drift. As shown in Figure 3.3, they found radiance to vary with spectral region (Hemmer, 1997). The VNIR region is unstable at both ends, while the SWIR 2 region is unstable near 1800 nm and simply runs out of energy from the calibrated radiation source used in the test at about 2400 nm. The SWIR 1 region, on the other hand, is extremely stable, and the ASD radiometric correction program (PCORRECT) makes use of this behavior to correct the VNIR at 1000 nm and the SWIR 2 region at 1800 nm. Because the SWIR 1 detector is temperature-controlled, it acts as a very stable anchor for most of the spectrum, even under thermal stress in the field. Thus, the factory calibration can be used under field conditions with the ASD radiometric error correction program. The shortest wavelength region of the VNIR does not, however, profit much from this approach. Unlike the drift in the other regions, which is due to changes in detector sensitivity, the drift in the blue is due to changes in the dark current associated with temperature effects on the electronics. Thus, to achieve maximum accuracy of radiance measurements in the VNIR, and particularly the blue, frequent dark current corrections are recommended, which should solve the problem. The author had intended to illustrate corrected radiance measurements with the ASD FieldSpec® FR, using the PCORRECT program and dark current correction, but the instrument

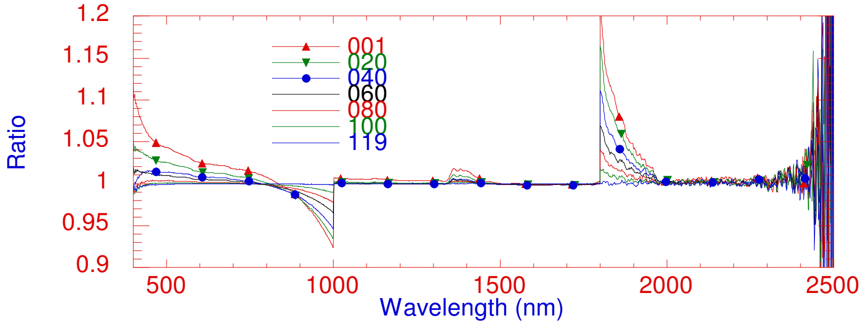

Figure 3.3. Uncorrected sensitivity drift of the FieldSpec® FR, shown by the ratio of spectrometer response at various times to the response at 120 minutes. Thus, the greatest error is shown at time 001. Times are relative to the start of the experiment, rather than ASD FieldSpec® FR power up (from Hemmer, 1997).

malfunctioned. Interestingly, the instrument malfunction was, at first, sufficiently subtle that relative reflectance measurements were not apparently affected. Thus, the ability of the instrument to make repeatable radiance measurements in the laboratory using a constant source are a sensitive test of instrument performance. As pointed out in Section 5.2.1, users who are interested in measuring radiance, but unable to gain access to a calibrated uniform source, should be able to find out if they have a problem by using any constant light source, preferably on a regulated power supply, and a white reference.

In addition to frequent dark current corrections during radiance measurements, use of a tripod and leveling device, or some other method to assure constant geometry, is also recommended to increase both accuracy and repeatability (see below).

Repeatability of Measurements. The fiber optic cable provides the ability to quickly and easily point the spectrometer field of view at different targets, especially when using the pistol grip. However, several users noted that flexure of the cable can change the apparent reflectance of a target by changing the signal level. Buntzen (1996) measured this effect by recording the digital number (DN) level with the cable coiled vs. the cable extended, while viewing a constant source. He found the flexure effect, even in this extreme flexure case, to be quite small. The ratio of DN extended to DN coiled yielded a negative fractional difference of up to 3% at the extreme short wavelength end of the VNIR (350 nm), and only about 1% at 400 nm. Most of the VNIR was flat, but the SWIR 1 region showed a 0.5-1% positive difference, while the SWIR 2 region showed a positive 2% difference. Other users have reported larger changes with cable flexure, but this may be due more to tilting of the optical head of the fiber optic cable than to cable flexure. In this case, a slight tilt of the optical head associated with testing cable flexure can make a significant difference in signal level associated with BRDF variations of target and/or reference. In any case, mounting the pistol grip on a tripod, and thus immobilizing both optical cable and field of view, is recommended for reflectance measurements requiring high repeatability and accuracy. In this configuration, the most convenient way to measure the reference is to superimpose reference on target, or replace target with reference, in the fixed field of view of the instrument. If the tripod must be moved between measurement of target and reference, a compass and level bubble shoud be used to make sure the geometry of measurement has not changed.

Jim Crowley of the U. S. Geological Survey and Tim Bowers of Earth Satellite Corp. made ten reflectance measurements of kaolinite with a fixed pistol grip under laboratory conditions to demonstrate the repeatability of ASD FieldSpec® FR spectra under ideal conditions. They took ten spectra (average of 40 scans), 15 seconds apart, using the same reference. When individual spectra were compared to the average of all ten in the 400-2500 nm range, the mean deviation from the average was less than a tenth of one percent, and the maximum deviation averaged just over half a percent, showing excellent repeatability. The largest deviation from the average was displayed by the first spectrum. This is so common with all field spectrometers that measuring spectra is like cooking pancakes: be prepared to throw away the first one.

Field of View (FOV). As described above, the optical cable is composed of bundles of fiber optics, with different bundles serving different detectors. Thus, it is inevitable that different detectors will have substantially different fields of view, especially with narrow FOV foreoptics. In his preliminary measurements, which did not fully reveal the extent of the problem, Hemmer (1997) nonetheless found relatively little FOV overlap for the different detectors using 5° foreoptics. This has significance for measurements of reflectance from heterogeneous targets, where different detectors may be measuring reflectance of significantly different surfaces. Users need to know how the size of spectrometer FOV changes with different foreoptics and distance from the target, so that they can select these parameters to assure representative measurements. In any case, averaging multiple measurements of a target is a good practice to compensate for heterogeneity (which may be too subtle for the eye to note), and so that scans with spectral artifacts (see below) can be discarded.

Spectral Artifacts. A few users have noted an occasional sinusoidal modulation of the spectrum in the SWIR 1 region, which Buntzen (1996) referred to as "ringing." This modulation can reach the 2-3% level, and so can be a significant spectral artifact, introduced presumably by the instrument's electronics. ASD points out that, more commonly, when an artifical light source in the laboratory is within one meter or less of the target, an optical interference effect can cause this modulation unrelated to instrument electronics. The author does not fully understand this effect, but presumes it is a beat frequency between the 60 hz frequency of the lamp and the scan rate in the SWIR. If such a modulation is seen in the laboratory, the light source should be moved back from the sample and the measurement repeated to determine if this is the cause.

A more common artifact is a reflectance offset that may occur between the different detector ranges at 1000 and/or 1800 nm. Poor observational technique does tend to exaggerate the offsets. For example, measuring the target and reference at different solar-sample-spectrometer geometry, especially upsun and downsun, will lead to reflectance offsets more often than not. Reflectance offsets may also be a signal that it is time to store a new reference spectrum.

One might think that spectra on the computer screen could be monitored for these spectral artifacts and rejected for archiving. Unfortunately, the FieldSpec® FR archives the next spectrum measured, not the one on the screen. Thus, digital data recorded in the field must be winnowed by inspection of each spectrum to delete bad data.

3.3 GER 3700 by Geophysical and Environmental Research Corp.

3.3.1 Instrument Description

The GER 3700 spectroradiometer (Figure 3.4a) is a single-beam instrument that combines three spectrometers to cover the wavelength range from 350 to 2500 nm. Fixed gratings and linear arrays make for the reliability and ruggedness of non-moving optics. A 512 channel Si array covers the range from 350 to 1050 nm, a 128 channel PbS array covers the range from 1050 to 1850 nm, and a 64 channel PbS array covers the range from 1850 to 2500 nm. These arrays result in average sampling intervals of 1.5 nm in the VNIR, 6.2 nm in SWIR 1, and 9.5 nm in SWIR 2 (but see Tips section below). Incoming radiation is chopped for the PbS detectors. Recording a single spectrum takes about 1.0 sec, including dark current correction. Good signal-to-noise is accomplished by averaging measurements (traditionally referred to as "scans," even by GER, although this is a non-scanning instrument). The default setting results in 4 scans. However, for a typically illuminated target, 8 or more scans are usually averaged to obtain good signal-to-noise, although this appears to vary somewhat from instrument to instrument. Averaging 8 scans takes about 12 seconds when the spectrum is displayed, and 7 seconds if the spectrum is written directly to disk without a display (occurs with neither option checked in the OPTIONS menu of the Windows-based program used for computer control of the instrument). Averaging 16 scans takes about 17 seconds with display, and 14 seconds without.

Figure 3.4a. GER 3700 in its more common configuration on a tripod (Photograph courtesy of Tom Corl, GER).

The standard radiation input to the GER 3700 is through a foreoptic with a 3° FOV (10° optional). This foreoptic is fixed to the housing of detector arrays and associated electronics, making an instrument too heavy (6.4 kg) to be hand held under most circumstances. Instead, a tripod is usually required to hold the spectrometer in position for spectral measurements, as illustrated in Figure 3.4a.

Figure 3.4b. Tom Corl carries the GER 3700 spectrometer in backpack with fiber optic cable (Photo courtesy of Tom Corl, GER).

The manufacturer lists a fiber optic cable with a 23° FOV as an option, which would present the "point-and-shoot" convenience of the ASD FieldSpec® FR. Apparently, this option was little used in the past because the energy throughput of the cables was too low for most applications. The manufacturer reports that new cables have much better performance, in which case the spectrometer can be placed in a light backpack instead of on a tripod, and the instrument becomes much more portable (see Figure 3.4b). As with all fiber optic cables, attenuation increases with increasing wavelength, and users should evaluate cable performance for their application(s) before selecting this potentially useful option.

When using the 3° FOV foreoptics in tripod mode, the instrument is aimed by use of a laser beam sight for nearby targets, and a telescopic sight for faraway ones. The sights are mounted on the side of the spectrometer, resulting in a slight offset between the sight center and the instrument FOV. The instrument is controlled, data displayed in real time, and stored using a sub-notebook computer (3 kg for the Rocky) attached to the spectrometer by an electrical cable that can be up to 15 m long (see Figure 3.4a). The computer is powered by its own internall battery, while the spectrometer is powered by a 12v Gel cell (2.4 kg).

As discussed above, spectral resolution is difficult to define, and GER specifies sampling interval, but not resolution, for the 3700. Figure 3.5a shows that this instrument cannot detect the kaolinite doublet near 1400 nm, and Figure 3.5b shows that the distinctive polyester spectral triplet in the 2200-2300 nm region is just barely resolved. Considering the 20 nm gap between the kaolinite bands, and the 25 nm gap between the polyester bands, the spectral resolution of this instrument appears to be poorer than 20 nm in the SWIR 1 region, and about 25 nm in the SWIR 2 region. Users will need to determine if this spectral resolution is compatible with their application(s). Some users, such as those interested in the broad bands of vegetation for species identification or water stress estimation, or ground truth measurements for multispectral satellite data, may even accept still lower resolution in the SWIR. These users should be aware of the existence of the less complex and less costly GER 2600, which covers the entire SWIR range with a single detector array.

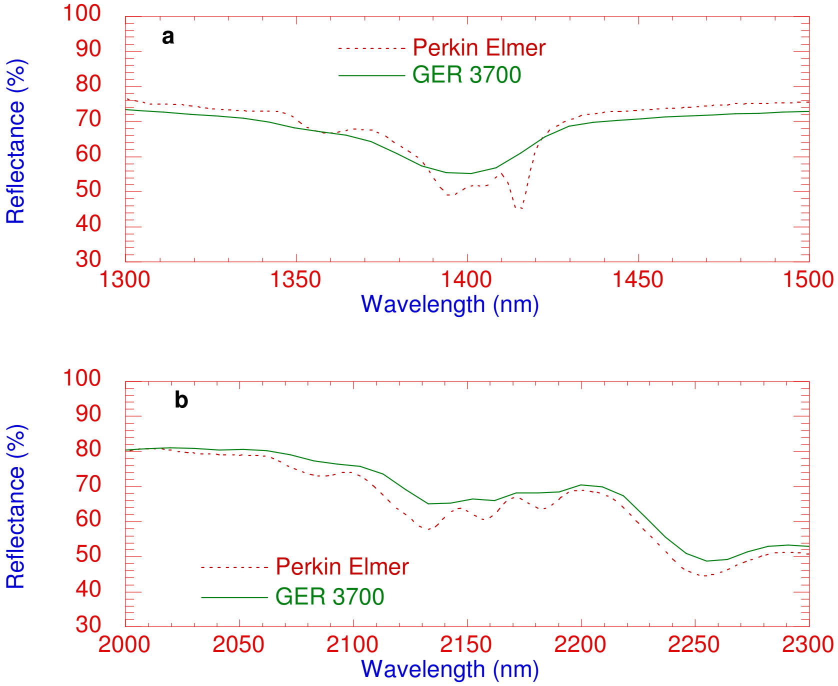

Figure 3.5. Comparison of reflectance spectra of kaolinite (a) and polyester fabric (b) measured by a Perkin Elmer Lambda 900 laboratory spectrometer and the GER 3700 under laboratory conditions. (Perkin Elmer spectra by Jim Crowley, U. S. Geological Survey; GER 3700 spectra by Ponder Henley, U. S. Army Corps of Engineers Topographic and Engineering Laboratory).

Table 2. GER 3700 manufacturer's specifications as of December, 1997 (comments in parentheses are the author's).

Spectral Range	350 nm to 2500 nm
Spectral Sampling	1.5 nm over the range 350-1050 nm 6.2 nm over the range 1050-1850 nm 9.5 nm over the range 1850-2500 nm (Sampling intervals given are averages. See Tips section for variations in spectral sampling interval with dispersion angle, especially in the SWIR.)
Data Interval	Not specified (Data interval, like the sampling interval, varies with dispersion angle).
Spectral Resolution	Not specified (see Fig. 3.5 and text).
Field of View	3° fixed foreoptic standard 10° fixed foreoptic optional 23° fiber optic cable optional
Scan Time	0.5 seconds for a single scan (8 to 16 scans are usually averaged in measuring the reflectance of a typical target for good S/N).
Power Source	External rechargeable Gel cells for spectrometer. Computer powered separately by internal battery consistent with model selected.
Size	Spectrometer head 28.6 x 30.5 x 11.4 cm. Computer 29 x 24 x 6 cm
Measurement type	Single beam bidirectional, requiring either a solar or artificial external light source.

Weight	Spectrometer head 6.4 kg Battery 2.4 kg Computer (3 kg for the Rocky, but any Windows-compatible computer will do) Cables ~0.5 kg (Operational use typically requires a tripod ~ 2 kg, unless the optional fiber optic cable can be used. The spectrometer carrying case supplied weighs 4.6 kg, but can be replaced by a light backpack.)

3.3.2 Instrument Tips and Rules of Thumb

Sensitivity Drift. GER makes no pretense that the 3700 is marketed primarily as a radiometer. For example, they quote a radiometric calibration accuracy (between 10° and 30° C) of ± 5% at 400 nm, ± 4% at 700 nm, ± 5% at 1000 nm, and ± 7% at 2200 nm, because the factory calibration is performed at room temperature only. The use of uncooled detector modules precludes accurate radiometry under the thermal stress of typical field conditions without user calibration of the instrument at different temperatures. Buntzen (1996) measured radiance errors at room temperature generally consistent with the manufacturer's specifications out to 1900 nm. Beyond that wavelength, however, the radiance error increased rapidly to 20-25%. In addition, the factory calibration resulted in a variable error curve, making it impossible to apply a simple correction coefficient. GER suggests that this may have resulted from use of an older instrument in need of a repeat factory calibration.

Michael Schaepman, of the University of Zurich points out, however, (personal communication) that the GER 3700 data output has the advantage of presenting both raw target radiance and detector operating temperatures in each digital record. This raw data allows the user to calibrate instrument responsivity at different operating temperatures in the laboratory, instead of relying on a factory calibration. With this approach, the University of Zurich has successfully used the GER 3700 for spectral radiometry in the field.

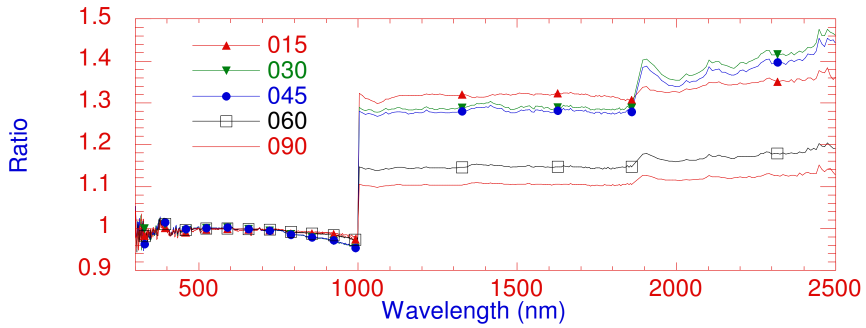

Figure 3.6a. Uncorrected sensitivity drift of the GER 3700 shown by the ratio of spectrometer response at various times to the response at 120 minutes. Thus, the greatest error is shown at time 015. Times are relative to the start of the experiment, which was shortly after GER 3700 power up. Note that the Y-axis scale has been expanded compared to that of Figure 3.3, and the X-axis has been extended to 300 nm in this figure, compared to the 400 nm limit of Figures 3.3 and 3.6b, to accommodate the legend. Data below 400 nm are noisy due to lack of signal. Radiance measurements by Ponder Henley, TEC, using a uniform source similar to that used by Hemmer (1997).

The sensitivity drift of the GER 3700 can be compared to that of the ASD FieldSpec® FR by comparing Figure 3.6a below with Figure 3.3 (note Y-axis scale change). In both cases, measurement procedures recommended by the manufacturers were deliberately not followed. That is, radiance measurements were made during instrument warm-up (instead of afterward) to simulate the thermal stress of field use, and no correction algorithm was applied, so that the extent of uncorrected sensitivity drift could be seen. One unfortunate result of this "hands off" approach is that the ASD FieldSpec® FR data were not corrected for dark current, while the GER 3700 automatically corrects for dark current with each measurement.

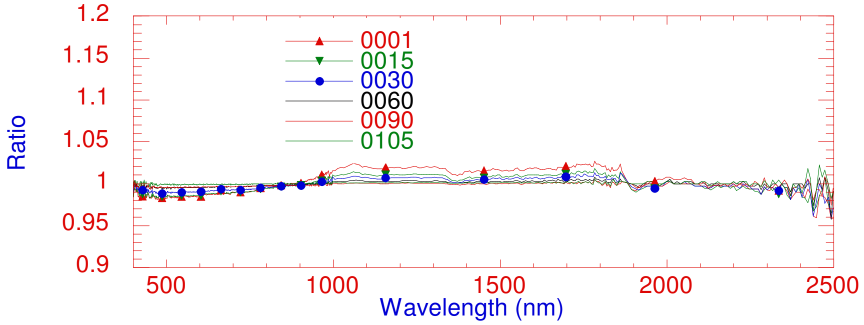

Figure 3.6b. A second series of drift measurements with the GER "detector matching" correction algorithm applied. Measurements were on a different day from those shown above and, again, began shortly after GER 3700 power up. Radiance measurements by Ponder Henley, TEC.

Comparison of Figure 3.6a with Figure 3.3 shows that the uncooled PbS detector arrays in the GER instrument vary relatively greatly in responsivity with temperature, which would be expected for uncooled detectors, while the silicon array response of the GER remains relatively stable.

The relative stability of the VNIR range for the GER 3700 is the basis for the "detector matching" option in the GER 3700 software, the effect of which is shown in Figure 3.6b. This option matches the SWIR to the VNIR in either radiance or reflectance, eliminating the common offset between detector arrays, and taking advantage of the greater stability of the VNIR. This detector matching option is now the program default on new instruments, and a change of program default to this option is recommended for older machines. As is the case with most instruments, allowing the instrument to warm up before use is also recommended.

Repeatability of Measurements. Under ideal laboratory conditions, the GER 3700 provides good repeatability. Based on Ponder Henley's measurements of a 50% reflectance standard, the mean deviation of individual spectra from an average of ten was 0.19%, and maximum deviations averaged 1.49%. This precision is a factor of between two and three worse than that exhibited by the ASD FieldSpec® FR, but users having both instruments uniformly stated that GER measurements in the field had higher precision. This observation is probably related to the manner of measurement. The GER 3700 is usually used with a tripod, while the ASD FieldSpec® FR is typically used in the point-and-shoot mode made possible by its fiber optic cable, and in this mode differences in solar-sample-instrument and solar-reference-instrument geometry probably dominate the error budget.

Spectral Resolution. Although spectral resolution of the GER 3700 is illustrated in two wavelength regions in Figure 3.5, potential users should check the data interval in their wavelength range of interest. Presumably the data interval represents the detector array configuration relative to the dispersed spectrum, and hence the sampling interval, and this interval varies within the wavelength ranges of the three arrays. For example, for Ponder Henley's instrument, the data interval in the VNIR varies between 1.5 and 1.6 nm; the interval in the first SWIR range shrinks progressively from 9.5 nm at the beginning to 4.8 nm at end; and the interval in the second SWIR range also shrinks from 11.9 to 8.7 nm from beginning to end. Such a variation in sampling interval implied by these variations in data interval also implies variable spectral resolution. Note that, since each GER 3700 is essentially custom built (typical of all field spectrometers), sampling intervals may vary from instrument to instrument.

Software. The Windows software supplied with newer GER 3700 instruments is user friendly with a number of useful applications. The older, DOS version of the software controlling the spectrometer does, however, have two advantages over the newer, Windows, version. First, it supports a monochrome screen, and second, it is faster because of the computational overhead of Windows, especially for a slower computer. One confusing variation between the two programs is worth noting for users changing from one to the other. When scan averaging is used in the DOS version, the number selected is the number of scans averaged. When scan averaging is used in the Windows version, the number of scans averaged is two raised to the n-1 power, where n is the number selected. Thus, a scan averaging of 5 is two to the fourth power, or 16 scans.

3.4 GER Mark V by Geophysical and Environmental Research Corp.

3.4.1 Instrument Description

Unlike any of the other field spectrometers, the GER Mark V is a double-beam instrument, meaning that it simultaneously views both target and reference, so that changing irradiance levels can, in principle, be completely compensated for during a reflectance measurement. Under changing light conditions, this is a major advantage over the other, single-beam instruments, which must alternately view target and reference.

The spectroradiometer system is designed with three gratings on a single stepper motor-driven mount. As the grating module is rotated, the instrument covers the spectral range from 300 nm to 3000 nm with one continuous scan that takes 30 to 60 seconds. Order sorting filters and detectors are changed automatically to accommodate the large wavelength range. The target and reference beams are modulated by the same tuning fork chopper and are directed through the same optical system to two separate detector modules containing Si and PbS detectors. The detector modules are mounted in a sealed, thermoelectrically-cooled housing. Cooling provides relative radiometric stability and high signal-to-noise ratios, even while operating in extremely hot environments.

Figure 3.7. Photograph of the GER Mark IV, the optical head of which is virtually identical to the Mark V. MTL Systems solves the tripod mobility problem with wheels during measurement of large calibration panels for an aircraft sensor overflight.

The dual fields of view can be seen through the same input optics used by the spectroradiometer, making aiming of the instrument more accurate than for most field spectrometers (but see Tips section below). Each field of view is an oblong, nominally 6° wide and 4° high, resulting in side-by-side viewing of target and reference panel.

The spectrometer is controlled by a laptop computer, which is carried, along with battery and electronics, in a fitted case separate from the optical head. Simple, menu-driven programs control the setup, acquisition, and data storage and manipulation functions. The electronics/computer case and the optical head are connected by electrical cable. The optical head is sufficiently heavy that it must be mounted on a tripod for measurements (see Figure 3.7).

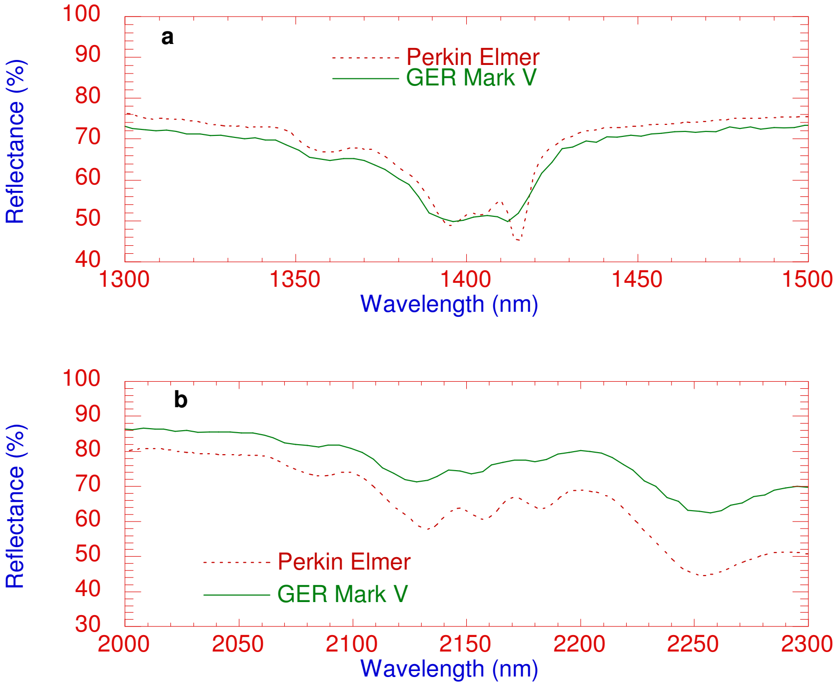

Figure 3.8. Comparison of reflectance spectra of kaolinite (a) and polyester fabric (b) measured by a Perkin Elmer spectrometer and the GER Mark V under laboratory conditions. (Perkin Elmer spectra by Jim Crowley, U. S. Geological Survey; GER Mark V spectra by Tom Corl, GER).

The entire instrument is very ruggedly constructed, as if to military specifications. Many of the Mark IV spectrometers, the previous and virtually identical version of this instrument, are still in use around the world, despite being over ten years old. The major difference between the Mark IV and the Mark V is that the older version used a rugged and temperature-tolerant control box/data logger for control of the instrument and recording of data, while the Mark V uses a modern laptop computer (which, in the case of the Amrel Rocky, can be almost as rugged as the old control box).

Spectral resolution of the GER Mark V is better than that of the GER 3700, as illustrated in Figure 3.8. The kaolinite doublet near 1400 nm is just resolved (Fig. 3.8a), and the polyester features between 2100 and 2200 are slightly better resolved (Fig. 3.8b). Thus, spectral resolution appears to be about 20 nm in both of the SWIR regions.

Table 3. GER Mark V manufacturer's specifications as of December, 1997 (comments in parentheses are the author's).

Spectral Range	350 and 2500 nm
Spectral Sampling	2 nm over the range 350-1050 nm 4 nm over the range 1050-2500 nm
Data Interval	2 nm in the 350-1050 nm range 5 nm in the 1050-2500 nm range
Spectral Resolution	Not specified. (See Fig. 3.8 and text.)
Field of View	Dual FOV 6° x 4° (but see Tips section).
Scan time	Programmable from 30 sec up (typically 60-120 sec for good S/N).
Power Source	Rechargeable Gel cells
Size	14.5 x 25.5 x 25.5 cm (spectrometer head only).
Measurement type	Double beam bidirectional, requiring either a solar or artificial external light source.
Weight	Spectrometer head 6.4 kg Battery 1.8 kg Computer (IBM-compatible, 1-3 kg) (Operational use also requires a tripod, ~ 2 kg, and cables, ~0.5 kg. A padded field case supplied for the computer weighs 5 kg, but can be replaced by a light pack.)

3.4.2 Instrument Tips and Rules of Thumb

Dual Beam Plus and Minus. This is the only double-beam instrument available, and its slow scan rate is a penalty that may be worth paying if spectral measurements must be made under highly variable light conditions. However, because different detectors are used for the two beams, individual detector calibration becomes an important factor in accuracy. MTL Systems, Inc. has used its (upgraded) Mark IV to measure absolute radiance in cooperation with other organizations using specialized instruments for this purpose. They found that detector sensitivity varied by only about ±1.5% in absolute radiance during a field day, because the detector modules are temperature-controlled. However, a calibration (including the factory calibration) cannot be expected to last for weeks or months, because detectors age, even without the stress of field use. Radiance accuracy in the 1% range requires a field-portable calibrated lamp and integrating sphere (see Fig 5.2).

One way to check on the extent of the potential detector calibration problem is to make two measurements with first the reference and then the target in the target field. By ratioing the target radiance output in the two measurements, a reflectance spectrum is obtained using the same detector. Comparison with a reflectance spectrum measured in normal double-beam mode with the two detector modules shows the magnitude of detector calibration error, if any. Note, that one of the advantages of the GER instruments is that they do provide data on both target radiance and reference radiance in each digital record.

A second potential problem with this dual beam design is possible radiation scattering between the two beams. MTL Systems, Inc. found that 1-2% of reference beam energy falls on the target detector for their Mark IV, and the Mark V uses the same optical design. This can introduce a relatively small error in reflectance or radiance measurements that may be significant for some applications aiming for very high accuracy. Measuring the reflectance of a dark target using both a bright and a dark reference (e.g., 99% and 2% calibrated Spectralon® panels) will determine the extent of the problem, if any, with a particular instrument. If such a problem exists, the effects can be avoided in two ways. First, a reference material can be used with a reflectance close to that of the target. More conveniently, perhaps, the instrument can be used in single beam mode, as above. If both fields of view are filled alternately with target and reference, reflectance spectra of two adjacent areas on the target can be obtained.

Aiming Optics. Sighting target and reference through the spectrometer optics is a definite advantage, but the sighting optics have a significant parallax problem. This means that care must be taken to hold the eye on the optic axis, or the apparent locations of target and reference fields can shift. Further, the locations of these target and reference fields need to be checked periodically, to make sure that the optics themselves have not shifted due to hard field use. This is accomplished by monitoring the signal level at a single wavelength, while moving a bright source into the field of view sequentially from the top, bottom and sides.

3.5 The Pima II by Integrated Spectronics Pty. Ltd. of Australia (U. S. Source is Spectral International, Inc. of Arvada, CO)

3.5.1 Instrument Description

As pointed out in the Background section, solar irradiance declines rapidly in intensity through the SWIR, and is strongly absorbed by water vapor in the atmosphere. While passive spectrometers can be designed to handle the low energy, there is no way to completely eliminate spectral artifacts caused by water vapor absorption. Yet, for many applications, clean spectra of the target materials free of atmospheric artifacts are very desirable (e.g., for developing a spectral search library). We include the PIMA II in this report because it is an active instrument (uses its own internal radiation source) that obtains very high quality spectral data in the region (1300-2500 nm) most affected by water vapor absorption bands, which also typically contains the most useful spectral data.

Figure 3.9. The PIMA II field spectrometer, showing a sample being brought to the measurement window by Jim Crowley, U. S. Geological Survey.

The PIMA II uses a single grating to scan its limited wavelength range in 20 to 60 seconds, depending on the sampling interval selected. The dispersed spectrum is scanned across a slit entrance aperture to an integrating sphere, which has a window port on the opposite side through which the target is illuminated. A thermoelectrically-cooled PbS detector at another port in the sphere detects the energy reflected from the target at each wavelength interval. The radiation source, grating, small integrating sphere, detector, electronics, and palmtop computer are all contained in a hand-held field case about the size of a shoe box (see Figure 3.9).

Since spectra are measured by illuminating a target material through a window in the side of the instrument, either the target must be moved to the window, or the instrument held to the surface of the target. The spot size illuminated is quite small (2 x 10 mm), so that numerous measurements must be made to spectrally characterize a heterogeneous surface, and some targets, such as a vegetative canopy, do not lend themselves to this kind of measurement at all.

The instrument is currently controlled by a Hewlett Packard LX200 palmtop computer, which stores data on removable SRAM memory cards, with data retrievable to an IBM-compatible PC via an RS-232 port. Menu-driven software operates the spectrometer, and automatically tags data files with time and date. The instrument also has an interface for a portable GPS receiver, so that location

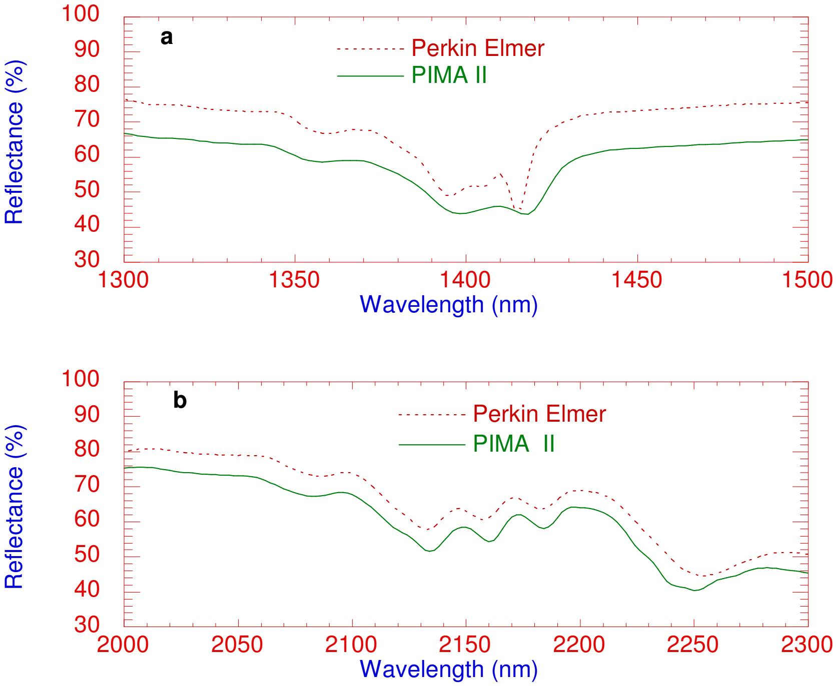

Figure 3.10. Comparison of reflectance spectra of kaolinite (a) and polyester fabric (b) measured by a Perkin Elmer Lambda 900 spectrometer and the PIMA II under laboratory conditions. (All spectra by Jim Crowley, U. S. Geological Survey).

can be recorded accurately. The spectrometer (4.5 kg) is powered by two rechargeable 6 v batteries (2.7 kg) worn in a fanny pack, while the computer is powered by two AA batteries.

Spectral resolution of the PIMA II is the best of all of the field spectrometers in the reflective region of the spectrum. As shown in Figure 3.10a, it resolves the kaolinite doublet slightly better than the ASD FieldSpec® FR, and the same is true for the polyester triplet in Figure 3.10b. The PIMA II spectrum in Figure 3.10b was measured with an older model of the instrument. The distortion in the spectral curve near 2250 nm is not seen in spectra recorded by more recent models.

Table 4. PIMA II manufacturer's specifications as of December, 1997 (comments in parentheses are the author's).

Spectral Range	1300-2500 nm
Spectral Sampling	2 or 4 nm selectable
Data Interval	2 nm
Spectral Resolution	Not specified (but see Fig. 3.10 and text).
Field of View	2 x 10 mm
Scan Time	20-60 seconds, depending on sampling interval selected.
Power Source	Two 6 v Gel cells in fanny pack
Size	26 x 15 x 15 cm
Measurement type	Contact directional hemispherical reflectance with an internal light source.
Weight	Spectrometer (including integral computer) 4.5 kg Battery pack 2.7 kg

3.5.2 Instrument Tips and Rules of Thumb

Sensitivity Drift. Dealing with an active instrument is much simpler than dealing with a passive one. Each spectral scan is radiometrically self-calibrating, and the instrument is virtually foolproof, providing that the target lends itself to being pressed against the spectrometer window. One recommendation is that the instrument be oriented so that the sun does not fall on its window side during measurement. The illuminating source is chopped, so that theoretically a dc source like the sun will not affect the output signal level, but a solar illumination effect has been reported.

Absolute Reflectance. The PIMA II is designed to measure near-absolute directional hemispherical reflectance, according to the manufacturer, the nearness being limited primarily by the necessarily small size of its integrating sphere. Our measurements show that PIMA II reflectance values are systematically slightly lower than highly accurate directional hemispherical reflectance measurements made with the Perkin Elmer Lambda 900 laboratory instrument (see Figure 3.10), which is consistent with the manufacturer's claim. Precision of measurement is also excellent. Ten consecutive measurements of the polyester fabric reflectance by Jim Crowley compared to their average showed a mean difference that averaged 0.16%, and a maximum difference that averaged 0.63%. Thus, directional hemispherical reflectance measurements with the PIMA are close to laboratory quality.

3.6 Pros and Cons of Instruments in the Reflective Region

3.6.1 Fast Single-Beam Instruments - ASD FieldSpec® FR vs. GER 3700

Transport. Both spectrometers can be deployed by one person, especially in the point-and-shoot mode using a fiber optic cable without a tripod. Two people are, however, recommended, with one to carry extra batteries and take notes and photographs, while the other takes spectra. If they use the same computers, the total weight of the GER 3700 is between 2 and 3 kilograms greater than that of the ASD FieldSpec® FR, even without the tripod normally used with the former. Thus, all other things being equal, the lighter ASD FieldSpec® FR is the field spectrometer of choice for applications in rugged terrain.

Fiber Optic Cable. The fiber optic cable intrinsic to the ASD FieldSpec® FR, offers an intuitive point-and-shoot method for acquiring many spectra very rapidly, which is probably why GER offers such a cable as an option for the GER 3700 (and GER 2600 as well). A fiber optic probe is a big advantage when trying to obtain the average reflectance of large targets, especially heterogeneous targets, because of the rapid data acquisition. However, it is also easy to become careless about solar-sample-instrument geometry during such rapid data acquisition, thus reducing reflectance accuracy and increasing the incidence of atmospheric and detector offset artifacts.

The convenient fiber optic cable has other drawbacks. Chief among these is the slightly different fields of view in different wavelength regions for the ASD FieldSpec® FR (not a problem for the GER 3700 or 2600). Another drawback is the reduced energy throughput of all fiber optic cables at longer wavelengths, especially for long cables. While the field of view problem may be ameliorated by placing an optical mixer in the foreoptics, there is a limit to how much further improvement can be expected in fiber optic transmission. Thus, applications can sometimes be difficult that require a distance greater than, for example, the 1.5 m between the optical head and the electronics/computer package of the ASD FieldSpec® FR. Such applications include mounting the optical head on a boom, goniometer, or helicopter skid. If the electronics package can be tolerated on the boom, goniometer, or helicopter skid, a solution to this problem exists. The ASD computer can be separated from the electronics package and located remotely, connected by a long electrical cable to the electronics package, just as a long electrical cable can be used to connect the spectrometer/optical head of the GER 3700 to its computer controller.

However, it is clear that careful thought must be given to the physical limitations implied by anticipated applications before ordering a field spectrometer, or requesting options or modifications.

Radiometric Accuracy. Both instruments will have changing sensitivity with changing instrument temperature, and the uncooled SWIR detectors of the GER 3700 are especially prone to sensitivity drift. The ASD FieldSpec® FR has temperature-controlled detectors in the SWIR, and its SWIR 1 range is highly stable as a result. Relying on this stability, ASD supplies a program to normalize the VNIR and SWIR 2 ranges to the central SWIR 1 range. The short wavelength end of the VNIR, and the long wavelength end of the SWIR 2 range are not, however, corrected by this approach, but dark current correction should, in principle, eliminate drift error in the blue.

The GER 3700 displayed an unusually stable response in the VNIR during instrument warm up on the laboratory, but must inevitably show sensitivity drift under thermal stress in the field. Unlike the ASD FieldSpec® FR, the GER 3700 generates digital records of spectra that include raw radiance and detector array temperatures. Thus, it can be calibrated in the laboratory for temperature effects on instrument responsivity. Properly calibrated for temperature effects by the user, the GER 3700 may provide better radiance data in the short wavelength range of the visible than does the ASD FieldSpec® FR, because it automatically corrects for dark current with every measurement. GER takes advantage of the VNIR stability by supplying a program to normalize the SWIR to the VNIR for both radiance and reflectance measurements. Because the changing SWIR response with temperature is not always uniform with wavelength (see Figure 3.6a), this correction decreases in accuracy with increasing wavelength away from the matching point

From these characteristics, it seems that a user-calibrated GER 3700 is best suited to radiometric measurements requiring high radiance accuracy in the visible, while the ASD FieldSpec® FR yields the most accurate data in the NIR/SWIR. For user calibration measurements, the GER 3700 offers the distinct advantage of including both the raw radiance values and detector temperatures in each digital record.

For those users unable to perform their own temperature calibration measurements, the ASD FieldSpec® FR offers the most accurate radiance data at all wavelengths under the thermal stress of field conditions.

Spectral Resolution. The two instruments appear to have about equal spectral resolution in the VNIR, but the ASD FieldSpec® FR has higher spectral resolution in the SWIR. The difference between 10 nm resolution and 25 nm resolution in this region may not be important for some applications, such as measurements of broad bands in vegetation spectra for species identification or water stess analysis, or ground truth measurements for multispectral satellite data. For most applications where material identification is important, however, the ability to resolve narrow molecular vibration bands in the SWIR is essential, making necessary the higher resolution of the ASD FieldSpec® FR.

Speed. In addition to providing higher spectral resolution data, the ASD FieldSpec® FR does so faster. It provides excellent signal-to-noise ratio spectra of the typical target in about 4 seconds, while the GER 3700 requires at least 12 seconds to acquire equivalent data (including display), which is important under field conditions of varying solar irradiance. Although the one minute time needed for periodic optimization of the ASD FieldSpec® FR must be factored into its overall speed estimate, it is still faster under typical conditions of use, when many spectra are being measured between optimizations.

The new and improved GER fiber optic cable option has not been tested for this edition. If its performance is typical of fiber optic cables, its energy throughput may be lower than that of the standard foreoptics, increasing scan averaging time for equivalent signal-to-noise.

Ruggedness. We do not have statistical repair histories on these instruments, and thus cannot say anything definitive about ruggedness. However, the author has been very impressed with the track record of the GER Mark IV, models of which are still in the field world-wide after ten to fifteen years. Like the GER Mark IV, the GER 3700 is ruggedly built, with heavy-duty Canon® electrical connectors, and heavy-gauge aluminum plates encasing the optical head, which is transported in a fitted and padded case. From its manner of construction, and considering the use of fixed optics, we tentatively conclude that the GER is the more rugged of the two instruments, and more likely to survive the rigors of repeated field campaigns, but only time will tell.

3.6.2 Double Beam Instrument - The GER Mark V

The GER Mark V is the only double-beam instrument currently available, and offers the great advantage of being able to compensate for rapidly varying solar irradiance, which can seriously degrade data from single-beam instruments (which may measure a single spectrum very quickly, but take time and key strokes to measure both target and reference). On the other hand, the GER Mark V is heavy, absolutely must have tripod support, and takes about 60 seconds to scan one spectrum. Moreover, since two different detector modules are used for the target and reference measurements, it offers a potential calibration problem. This potential calibration problem is small compared to the great advantage that the temperature-controlled detector modules offer for absolute radiometry. The relative stability resulting from this temperature control is a real plus for all applications requiring accurate measurements of radiance.

3.6.3 Active Measurement - The PIMA II

The PIMA II makes an active measurement using an artificial radiation source, which is the only way to obtain "clean" spectra in the SWIR free of atmospheric artifacts. The PIMA II is light, easy to use, and provides near-laboratory quality spectral data. It is used extensively by geologists, together with a library of mineral spectra and spectral search algorithms, to map mineral composition in the field. However, it has a wavelength range limited to the SWIR, cannot measure radiance, cannot measure targets from a distance, and has a very small measurement area. Ideally, this instrument would be used to complement measurements by one of the passive field spectrometers described above, by providing SWIR spectra free of atmospheric artifacts. On the other hand, active measurements avoiding atmospheric effects can be made with the passive instruments discussed above, given the electrical power and radiation source necessary to properly illuminate targets in the field.

4.0 INSTRUMENTS FOR THE THERMAL REGION

4.1 General

All of the spectrometers used in the thermal region use interferometric designs, and are commonly referred to as FTIR (Fourier transform infrared) spectrometers. Readers not familiar with this kind of instrument are referred to Griffiths and Haseth (1986) for more information.

As in the reflective region, only the instruments considered most useful (and most often used) have been reviewed here. One instrument not reviewed, for example, is the Illuminator by MIDAC Corp. of Irvine, CA. Like the two instruments reviewed, the MIDAC Illuminator is an FTIR spectrometer. Although the basic instrument is relatively inexpensive, this instrument was not reviewed because extensive (and expensive) customization is necessary to convert it into a radiometrically accurate field spectrometer, which requires a thermally stabilized enclosure and calibration blackbodies. As marketed, without customization, the instrument is field ready for detection of gases by uncalibrated absorption measurements. At last report MIDAC was not prepared to provide the customization necessary to convert the instrument into a spectroradiometer. Further, although ultimately transportable, it is both heavy (in the Bomem class) and power-hungry, although it does work on battery power. One user who has successfully customized a MIDAC Illuminator for radiometrically accurate field measurements of emissivity is Dr. Zhengming Wan of the University of California, Santa Barbara, who may be contacted for his comments by those interested in this option at wan@icess.ucsb.edu.

One of the instruments that is reviewed below is the microFTIR, produced by Designs and Prototypes. In evaluating the commentary on this and other instruments for the thermal region, the reader should be aware that the author played a key role in obtaining the grant and contract funding for Designs and Prototypes to develop the microFTIR. He also participated in the testing of the instrument during development. Thus, he has a paternal, but absolutely no proprietary, interest in the instrument.

4.2 The MD 104 by Bomem, Inc. of Quebec, Canada

4.2.1 Instrument Description

Bomem produces a line of FTIR laboratory spectrometers based on the familiar Michelson type of design, but using corner cube reflectors as the moving mirrors, which greatly reduces optical alignment problems. Corner cube motion necessary to produce an interferogram is achieved by rotating a balanced swing arm on a flex pivot bearing, resulting in mirror motion that is not affected by spectrometer orientation. This optical design is sufficiently rugged to allow use of these laboratory spectrometers in the field. One has even flown aboard the Space Shuttle.

Different Bomem spectrometer models cover a spectral range from 0.7 to 22 µm. One model, the MB104, is particularly recommended by Bomem for field use because it uses non-hygroscopic ZnSe optics. This instrument records spectra from 1.66 to 19.6 µm. Being basically a laboratory instrument, it must be customized for field use, and Bomem will perform that task. Unfortunately for purposes of generalization, these instruments are individually customized to match different intended applications, which means that there is no standard design. However, the Bomem MB104 used by MTL Systems is considered typical of such a field design for remote sensing applications, and will be used to illustrate instrument characteristics.

One unique aspect of the MTL Bomem design, when compared to the instruments reviewed above for measurements in the reflective region of the spectrum, is that the entire optical bench is heated to maintain the internal temperature of the instrument at 40.0±0.1 °C. Some kind of temperature control is necessary for any instrument to be used in the thermal infrared, because the instrument itself is a major source of infrared energy. Thus, the signal falling on the detector is composed in large part of instrument self-emission, which must be accounted for in order to make an accurate measurement of target spectral radiance. Unlike the reflectance region, where relative reflectance (compared to a standard) can be measured without an accurate measurement of radiance, calculation of emissivity requires an absolute target radiance measurement that can be compared to the radiance emitted by a black body at the same temperature.

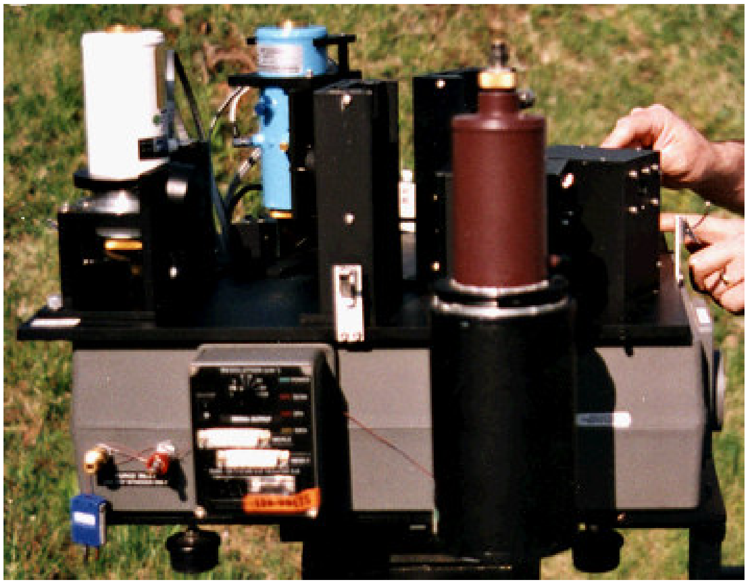

Figure 4.1. MTL Systems' Bomem MB104 optical bench.

The MTL Bomem accounts for instrument self-emission using the four-port (two input and two output ports) design of the MB104. A liquid nitrogen-cooled source is used at one input port to measure instrument radiance, which is subtracted during the measurement process from the total radiance. The responsivity of the instrument is calibrated using a black body at two different temperatures at the second input port, assuming a linear response between the two calibration temperatures.

The uncovered optical bench is shown in Figure 4.1, on which can be seen the blue dewar (pale gray in non-color editions) of the InSb detector used for the MWIR region, the white dewar of the MCT detector used for the LWIR region, and the red dewar (dark gray in non-color editions) of the liquid nitrogen-cooled cold source.

The instrument scans an interferogram (which can be transformed into a spectrum) each 1.2 seconds. These interferograms are co-added, or averaged, over whatever integration time is necessary to achieve the very high signal-to-noise (>1000/1) required to accurately calculate emissivity. This integration time varies with target temperature and spectral resolution. Using a 20° C blackbody as a target, this signal-to-noise can be obtained in about 30 seconds at 4 cm-1 spectral resolution and in about 2 minutes at 1 cm-1 resolution (the highest resolution of which the instrument is capable).

The MTL MB104 has a 2.6° field of view, with a 45° flat mirror in front of the entrance port that can be rotated 360° by a computer-controlled stepper motor. Thus, the instrument can view straight down, out to either side, or straight up, without moving the optical bench. However, there are no sighting optics, so that precisely aiming the field of view at a target on the ground is only approximate, making it desirable that the target substantially overfill the field.

An automatic data acquisition system measures and stores mirror temperature, instrument temperature, sample temperature (if measured by thermocouple), and atmospheric temperature, barometric pressure and humidity with each measurement data set. The information recorded not only documents the conditions of test, but also provides the means to model the radiometric environment and to derive compensations for atmospheric path transmittance and radiance when the spectrometer is distant from the target.

Bomem makes fine laboratory instruments. The principal disadvantage to fielding one is its weight. The optical bench alone weighs 44 kg, which necessitates a tripod or other supporting device of near equal weight. Figure 4.2 shows one configuration used by MTL Systems to enhance mobility of the instrument in the field. The dark gray optical bench can be identified by its white cover and the dewar of the cold source detector outside the cover. In front of the optical bench are the rotating foreoptics. Behind it is the data acquisition system (white, with a blue band in color editions), followed by a mast, which allows the spectrometer to be cranked up to a height of approximately 3.5 m. To the rear of the mast is an electronics rack which contains the blackbody temperature control box, and has the laptop computer controller for the spectrometer and foreoptics in a shock mounting on its top. The total weight of this mobile cart system is 381 kg, of which 236 kg is the weight of the cart and mast, and 45 kg that of the generator (not shown) necessary to provide the 150 W of AC power required to run the spectrometer.

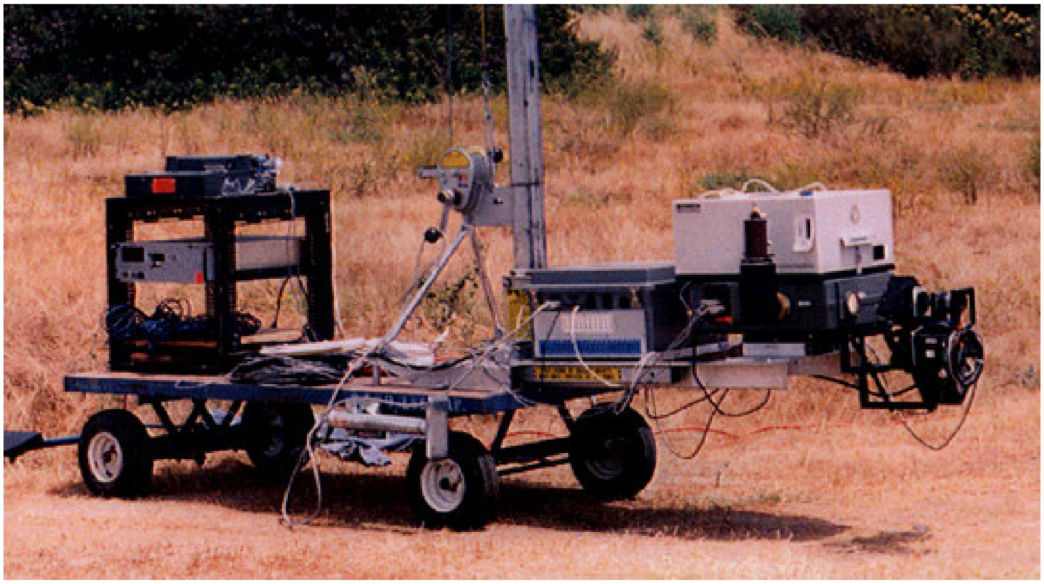

Figure 4.2. The MTL Systems Bomem MB104 on its field cart.

What has made such weight worth bringing into the field has been the relatively high spectral resolution achievable by the Bomem MB104, which is selectable from 1 wavenumber to 64 wavenumbers in 2X steps (i. e., 1, 2, 4, 8, 16, 32, and 64). The spectral resolution of all FTIR instruments is constant in wavenumbers, also known as reciprocal centimeters (cm^{-1}), because these instruments work in terms of frequency instead of wavelength. Unfortunately for comparisons with the performance of spectrometers that have resolution that is constant in wavelength, spectral resolution constant in wavenumber is variable in wavelength, becoming progressively worse at longer wavelengths. Thus, the

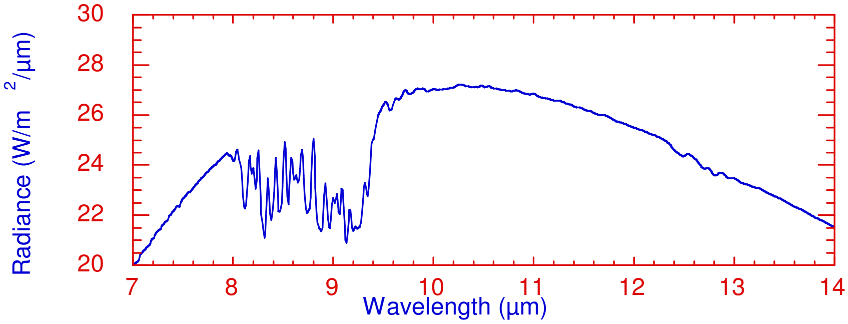

Figure 4.3. Spectral radiance of quartz sand measured with the MTL System Bomem MB104 under humid conditions in Dayton, OH, June, 1995. Spectral resolution was set at 4 wavenumbers. Measurement by Gary Petrick, MTL Systems.

spectral resolution in wavelength of an instrument with 1 wavenumber resolution is 0.0025 µm at 5 µm, and 0.01 µm at 10 µm. Fortunately, spectral resolution of FTIR instruments is easy to calculate from the length of mirror travel and precision of interferogram recording, and thus not normally a subject for dispute. Figure 4.3 shows a radiance spectrum of quartz sand recorded by the MTL Bomem MB104 set at 4 wavenumber resolution. The width of the water vapor emission lines reflected in the quartz reststrahlen bands is a good indicator of spectral resolution (compare the width of the same water vapor bands in downwelling radiance in Figure 2.11, which were recorded at 8 wavenumber resolution).

4.2.2 Instrument Tips and Rules of Thumb

Sensitivity Drift. Controlling the instrument temperature greatly reduces sensitivity drift, but does not completely eliminate it. Even when the optical bench temperature remains constant, which it rarely does in the field, the foreoptics are likely to change temperature, and they contribute to the self-emission. The MTL Systems data acquisition system, while not required for measurements, does give warning of such temperature changes, but the placement of thermocouples may not yield timely data. Consequently, blackbody calibrations are repeated at ten to fifteen minute intervals if highly accurate radiance measurements are desired.

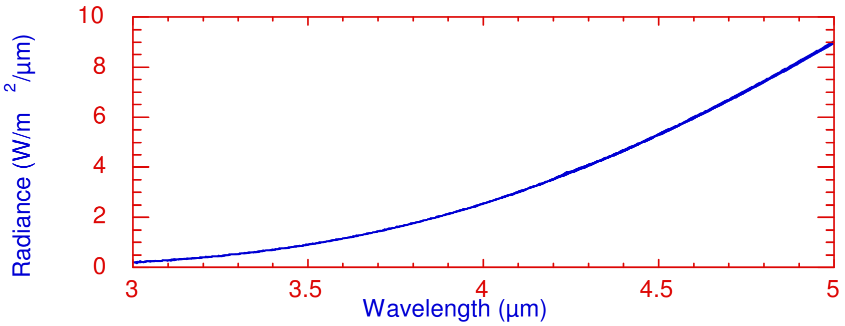

Figure 4.4. Comparison of a 30° C Planck function with four spectral radiance measurements of a 30° C blackbody by the MTL Systems Bomem MB104. All curves are so closely superimposed that they appear to be a single line. Measurements by Gary Petrick, MTL Systems.

Radiance Accuracy. Measurements of the MTL Bomem performance were made side by side with measurements of microFTIR performance under the direction of Andrew Korb, currently at SAIC, but then the author's graduate student at Johns Hopkins University. As illustrated by Figure 4.4, the repeatability of Bomem spectral radiance measurements is better than 0.05%, even in the low energy 3-5 µm region. With regard to accuracy, a convenient figure of merit is the accuracy with which spectral radiance measurements can be used to retrieve the temperature of a blackbody being measured. A temperature retrieval accuracy of 0.2° C was achieved with the laboratory measurements shown in Figure 4.4, which is considered excellent. Maintaining such accuracy in the laboratory or field, however, depends on the frequency of calibration to avoid the effects of sensitivity drift. Even in the relatively benign laboratory environment, temperature retrieval errors on the order of 1° C occurred two hours after calibration, and errors of 3° C occurred after three hours. In addition, the radiance curves departed progressively from a Planckian shape, and the combination of these errors resulted in significant errors in calculated emissivity.

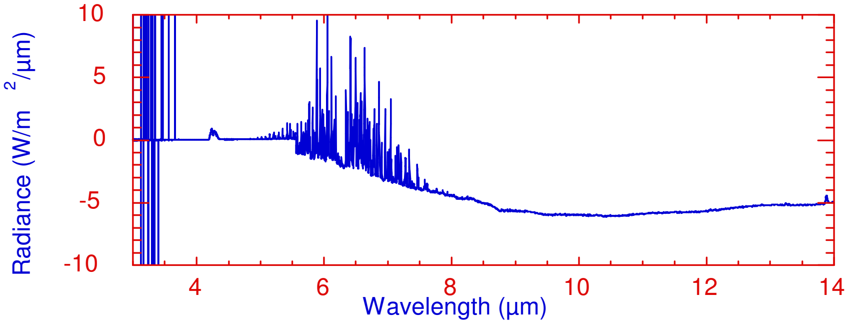

Figure 4.5. Spectral radiance measurement of a liquid nitrogen-cooled source with the Bomem MB104, using calibration blackbodies at 25° C and 65° C. Atmospheric CO_2 emission is seen near 4.2 µm, and water vapor emission lines are prominent between 5 and 8 µm. A combination of noise and water vapor emission occurs between 3 and 3.5 µm. Measurement by Gary Petrick, MTL Systems.

After timely calibration, measurements of blackbodies at temperatures between the two calibration temperatures show that the Bomem MD104 has a highly linear responsivity. Thus, no significant error arises from a linear interpolation between the two calibration temperatures. Not surprisingly, extrapolation of the calibration curve to very much lower temperatures than the lowest calibration temperature can be troublesome. Such an extrapolation is necessary when measuring downwelling radiance in the desert under clear sky conditions, where the lack of water vapor results in a sky temperature that is far below zero. To test the linearity of such an extrapolation, measurements were made of a liquid nitrogen-cooled source. Figure 4.5 shows that, although the instrument correctly recorded zero radiance in the 3-5 µm region, it incorrectly recorded significant negative values in the 8-14 µm region. A first order correction could be made when measuring a cold source by simply adding six watts of radiance in the LWIR. Other approaches are discussed briefly below in Section 4.3.2 and more fully in Section 5.3.2.

<u>Field of View.</u> With a field of view of 2.6°, the instrument should see a spot size 0.045 m in diameter at a distance of 1 m. However, measurements by Andrew Korb, SAIC, with a point hot source show that the actual spot size at that distance is 0.15 m, and that the fields of view of the InSb and MCT detectors are offset from each other by half that spot size. Overfilling the field of view with a target will take care of the first problem, as well as the difficulty of aiming the instrument. The offset of the fields of view in the SWIR and LWIR may give difficulty in measurements of heterogeneous targets.

Table 5. MTL Systems Bomem MB104 Specifications (author's comments in parentheses).

Spectral Range	6000-510 cm-^{1} (1.66-19.6 µm)
Spectral Sampling	N/A
Data Interval	0.05 cm^{-1} (at 1 cm^{-1} resolution)
Spectral Resolution	1 cm^{-1} to 64 cm-^{1}, selectable in 2 X steps
Field of View	2.6° (but see text)
Scan Time	1.2 sec (usually averaged for about 30 seconds at 4 cm^{-1} resolution-see text).
Power Source	Generator
Size	49 x 44 x 33.5 cm for optical bench

Weight	Optical bench 44 kg, generator 45 kg (see text for weight of optional supporting equipment).

4.3 The MicroFTIR by Designs and Prototypes, Inc.

4.3.1 Instrument Description

Like Bomem, Inc., Designs and Prototypes, Inc. has produced custom FTIR spectrometers with a wide variety of capabilities, including a high resolution (1 cm^{-1}) instrument to measure Fraunhofer lines in the visible, and other instruments that functioned in the SWIR, MWIR, and LWIR. They are currently working on an instrument that will cover the entire wavelength range from the visible through the LWIR at high resolution. However, the standard model that Designs and Prototypes has marketed for spectral measurements in the field, the microFTIR, or Model 101, is the instrument that will be considered here.

Figure 4.6a. Photograph of a microFTIR optical bench with a transparent Delrin cover. The sealed unit is filled with dry nitrogen to protect the KBr optics, with windows of ZnSe at entrance and exit ports. Foreoptics on the entrance port (left) allow viewing of the target through the same optics. The detector dewar on the exit port (right) contains both InSb and MCT detector chips in a sandwich configuration. (Figure from Korb et al., 1996.)

The nominal wavelength range of the microFTIR given by the manufacturer is 5000-666 cm^{-1} (2-15 µm), but the detectors and optics record valid data from 6410 cm^{-1} (1.56 µm) (the shortest wavelength allowed by the Nyquist frequency criterion) to 415 cm^{-1} (24 µm), given a hot enough source. The instrument uses a unique optical design that results in an extremely compact optical bench (see Figure 4.6a). While most readers may be familiar with the traditional Michelson moving mirror design, they are unlikely to be familiar with the microFTIR design, which was first described in detail only very recently (Hook and Kahle, 1996; Korb et al., 1996). Consequently, Figure 4.6b is included here as part of a brief explanation of this design, which is explained in detail in Korb et al. (1996). The heart of the interferometer is composed of two KBr prisms, separated by a minute air gap, which together form a hexagon. Instead of using individual mirrors and a beam splitter, optical coatings are applied directly to the prisms. The much denser packaging results in a very small size and a short optical beam path, greatly reducing growth of the field of view through the instrument. To take advantage of the optical compactness, a small laser diode is used instead of the common HeNe tube source as a frequency reference. Thus, the complete interferometer optical bench weighs just 0.8 kg.

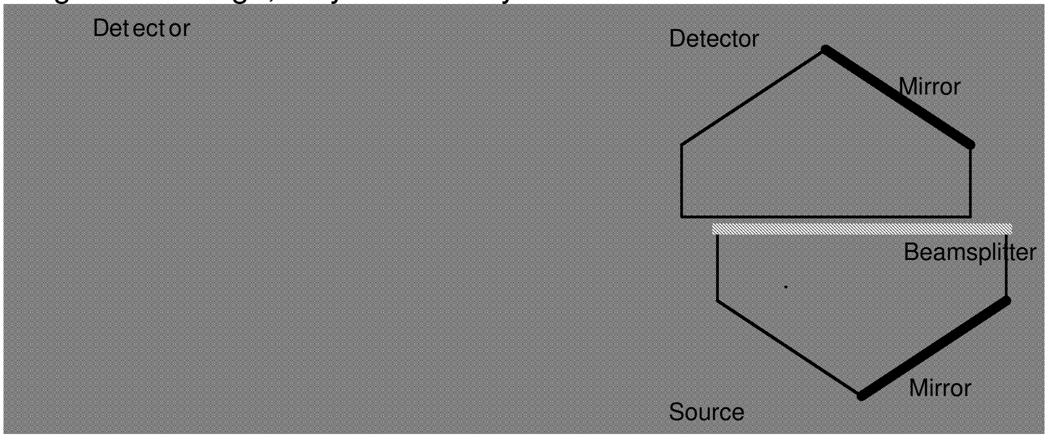

Figure 4.6b. Schematic of the microFTIR design, showing the path difference achieved by the offset of one of the KBr prisms. In practice, both prisms are offset in opposite directions to increase the path length difference. The drive effecting this offset is mass balanced to achieve a high tolerance of tilt, motion, and vibration (figure adapted from Korb et al., 1996).

Temperature control of the instrument necessary to account for self-emission is achieved by putting the optical bench into an insulated enclosure thermoelectrically maintained at a constant temperature, which can be set at 20±0.1 °C or 30±0.1 °C (25° C or 35° C for the JPL instrument shown below), whichever is closer to the external environment temperature. This thermal enclosure raises the weight of the optical head to 4.4 kg, which is small enough to be supported by a light tripod. The optical head is connected by a 5-m cable to an aluminum case containing the instrument electronics and notebook computer-controller (see Figure 4.7).

Both instrument self-emission and responsivity are calibrated with the common two-temperature approach, using a temperature-controlled blackbody. The blackbody temperature can be set to any of twelve temperature increments between 10 and 65 °C, with a temperature stability of ±0.1 °C.

Figure 4.7. MicroFTIR belonging to the Jet Propulsion Laboratory operational in Death Valley. Photograph by Simon Hook, JPL.

The microFTIR scans an interferogram each second, and a fast Fourier transform is performed in real time to produce a spectrum. These spectra are co-added, or averaged, to improve signal-to-noise, usually for 16 seconds for a room temperature target.

The foreoptics collect radiation into the interferometer with a 45°, off-axis, parabolic mirror mounted in a swivel head, so that the field of view can be pointed straight down, out to either side, or straight up. It has a focus from 1 m to infinity. When a 45° flat mirror is rotated into the optical train, this field of view can be accurately monitored in the visible via an eyepiece tube at right angles to the optical axis of the foreoptics (see Figure 4.6a). The standard foreoptic system is 2.5 cm in diameter and has a 4.6° field of view. An optional telescopic system is 5 cm in diameter and has a 2.3° field of view.

Spectral resolution of the microFTIR is 6 cm-^{1}, with a sampling interval of 3 cm-^{1}. In wavelength, 6 cm-1 resolution is 0.015 µm at 5 µm and 0.06 µm at 10 µm. Figure 4.8 illustrates this resolution with a radiance spectrum of the same quartz sand measured by the Bomem in Figure 4.3. These measurements were done side by side under the same atmospheric humidity and temperature conditions, and show the same water vapor bands reflected in the reststrahlen region. Comparison with Figure 4.3 shows that it is difficult to tell the difference between 4 cm-^{1} and 6 cm^{-1} spectral resolution in viewing these bands.

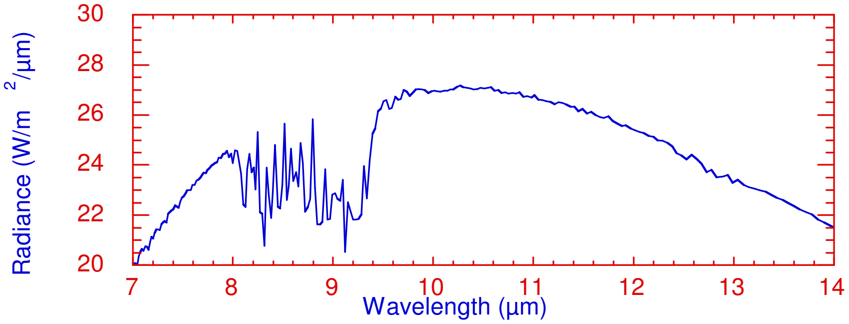

Figure 4.8. Spectral radiance of quartz sand measured with the microFTIR under humid conditions in Dayton, OH, June, 1995. Spectral resolution was 6 wavenumbers. Measurement by Andy Korb, SAIC.

4.3.2 Instrument Tips and Rules of Thumb

Sensitivity Drift. The microFTIR controls the entire instrument temperature to minimize sensitivity drift, and because instrument self-emission is a large fraction of total signal being recorded by the detector. Like all temperature-controlled instruments, it takes some time to come to thermal equilibrium, and it is strongly recommended that the thermoelectric heater/cooler be turned on one hour prior to instrument use, preferably using the automobile cigarette lighter attachment to save battery power. In the laboratory the instrument temperature is maintained to within 0.1 °C of the set temperature. In the field under intense desert sun, however, the instrument temperature may slowly rise by one or two degrees, and foreoptics are always subject to temperature change. Thus, re-calibration every ten to fifteen minutes is essential for acquisition of good data. Highest quality data requires re-calibration for every target measurement, especially when downwelling atmospheric radiance is varying rapidly (see Section 5.3.2).

Radiance Accuracy. Andrew Korb, SAIC, made side-by-side measurements with the MTL Systems Bomem, using the microFTIR on the same blackbodies and targets. He found equal performance of the two instruments in repeatability and radiance accuracy.

Like the Bomem, the microFTIR demonstrated excellent linearity of response, making a linear interpolation between calibration temperatures a valid assumption. Also like the Bomem, extrapolation of this calibration to very low temperatures posed problems. As shown in Figure 4.9, response to a liquid nitrogen-cooled target was correctly zero in the 3-5 µm region, but showed a significant incorrect positive anomaly near 12 µm. When the calibration temperature range was extended to lower temperature, the magnitude of the significant anomaly was reduced, and a smaller effect near 9 µm was eliminated, thus demonstrating clearly that this is, indeed, an extrapolation error (see Fig. 4.9). This has been experienced as a significant observational problem when measuring the downwelling radiance from a very clear, desert atmosphere with low water vapor content (Korb et al., 1996). A first order correction under such conditions would be to subtract radiance values obtained by contemporaneous measurement of a liquid nitrogen-cooled target. A more exact solution used by Johns Hopkins University is to use flame-sprayed brass as the diffuse reflecting surface for measurement of downwelling radiance. With an emissivity near 0.7, the brass plate self-emission (when heated by the sun) is sufficient to bring the total radiance measured into the linear extrapolation range, even with a very cold sky, as discussed more fully in Section 5.3.2.. The principal drawback to using a brass plate is that its temperature must be more carefully measured than is necessary for a diffuse gold plate, or for crinkled aluminum foil, because its self-

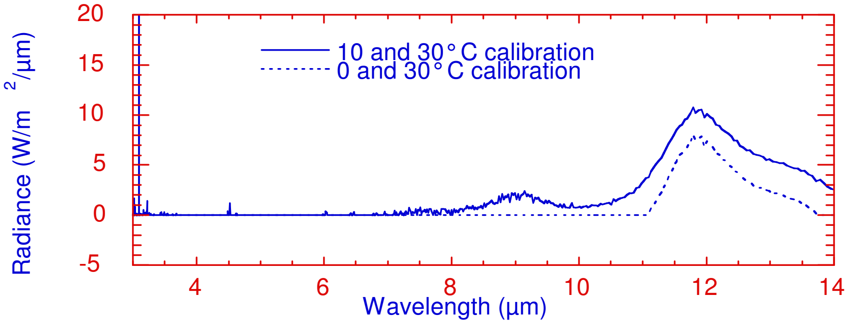

Figure 4.9. Spectral radiance measurements of a liquid nitrogen-cooled source with the microFTIR, using calibration blackbodies with different temperature ranges. Measurements were made closer to the boiling liquid nitrogen surface (and hence in a more nitrogen-rich atmosphere) than the measurement in Figure 4.5, accounting for less prominent atmospheric emission (from Korb, et al., 1996).

emission is so significant. In addition, brass tarnishes, which requires frequent cleaning and re-measurement of its directional hemispherical reflectance.

Field of View. With a field of view of 4.6°, the instrument should see a spot size 0.08 m in diameter at a distance of 1 m. Measurements with a point hot source by Andrew Korb, SAIC, showed that the spot size is very close to the theoretical prediction, probably one function of the highly compact optics (Korb et al., 1996). Further, because the InSb detector chip lies on top of the MCT chip, the fields of view of the two detectors coincide.

Table 6. MicroFTIR instrument specifications (author's comments in parentheses).

Spectral Range	5000-666 cm^{-1} (2.0-15.0 µm) (Nominal range, but full range with hot source is 6410-415 cm^{-1}, or 1.56-24 µm.)
Spectral Sampling	N/A
Data Interval	3 cm^{-1}
Spectral Resolution	6 cm^{-1}
Field of View	4.6°
Scan Time	1 sec (usually averaged for 16 seconds)
Power Source	2.5 kg 12 V battery in sling pack for spectrometer and blackbody (4 hr. operation). Computer independently powered.
Size	Optical head 25 x 25 x 20 cm Electronics/computer case 33 x 46 x 5 cm
Weight	Optical head 4.4 kg Electronics/computer case 7.55 kg (with computer) Battery 2.5 kg Light duty tripod 1.5 kg

4.4 Pros and Cons of Instruments in the Emittance Region

Spectral Resolution. One critical dividing line between these two instruments is maximum achievable spectral resolution. Some applications demand the 1 cm^{-1} resolution of the Bomem, such as remote sensing of many gases. For remote sensing of solids, liquids, and some gases, however, the 6 cm^{-1} resolution of the microFTIR is perfectly adequate.

The ability to vary the resolution of the Bomem for different applications is a decided advantage, especially when difficult observing conditions make it advantageous to use lower resolution to speed up the measurement process (see Section 5.3.2).

Transport. Another critical dividing line between these two instruments is transportability. The size and weight of the MTL Bomem MB104 and its ancillary equipment requires truck transport and a crew of at least two people for setup, while the microFTIR can be transported by hand and fielded by one person if necessary, although two is the optimum number. Applications using fixed sites may ameliorate the Bomem transportability problem. Applications requiring measurements in rugged terrain, frequent transport, and a small field party strongly favor the microFTIR, assuming that spectral resolution is not a deciding factor.

Pointing. The Bomem as fielded by MTL Systems is difficult to point accurately, although the reference laser spot can be used for locating the field of view on a nearby target, except in bright sunlight. No doubt Bomem, Inc. could devise an accurate pointing system using the spectrometer foreoptics like the microFTIR, but the offset of the fields of view of the two detectors remains a problem, unless the two-detector configuration is also changed to a sandwich detector. Again, a further customized Bomem could have much better pointing accuracy in all respects, but the standard microFTIR has excellent pointing accuracy as it stands.

Sensitivity Drift. It is obvious that the greater thermal mass of the Bomem will result in a more stable system temperature under the thermal stress of extreme heat or cold. In a laboratory or more benign environment, measurements of recovered blackbody temperatures showed no difference.

5.0 MEASUREMENT PROTOCOL

5.1 General

Details of measurement protocol depend strongly on applications of the data. Yet, the statement is often heard that spectral measurements in the field should be made simultaneously with sensor overflight if possible, or at least at the same time of day and under similar weather conditions. This statement arises out of the common use of field measurements to help calibrate and validate new airborne sensors. A moment of thought, however, suggests that this calibration/validation application should be necessary only very early in a sensor lifetime, and periodically as it ages. Ultimately, a hyperspectral sensor must independently produce reflectance spectra of surface materials, free of atmospheric and sensor response artifacts, for comparison with a spectral library. There will, of course, always be gaps in the spectrum where atmospheric water vapor is completely absorbing, and a spectrum acquired without some in-scene calibration may not represent absolute reflectance, but the shape of the spectral curve should be a valid representation of relative reflectance or emissivity. At such a stage, spectral measurements in the field may be used to better understand and interpret spectral variations in specific image cube scenes, or to provide a library of spectra for general interpretation of such data, or to identify and map specific materials at a spectral and/or spatial resolution not available from overhead sensors (such as the use of the PIMA II by geologists for mapping individual mineral abundances in hydrothermal alteration zones). Thus, the rationale for, and the use of, field measurements is changeable, and detailed measurement protocols will change accordingly.

If circumstances so alter cases, how then to write a section on Measurement Protocol? The author has chosen to emphasize the basics that are common to all spectral measurements, and develop generalizations that are valid for all, or most, applications. Certain applications are specifically referred to, such as overhead sensor calibration/validation. However, detailed measurement protocols supporting this application have already been written (e.g., HYMSMO Program Ground Truth Protocol, 1997), and the interested reader is referred to such a report for details.

5.2 First and Foremost, Know Your Instrument

It is surprising how many people go into the field without having first mastered use of their field spectrometer in the laboratory. The field is not an ideal location to develop that mastery, because too many variables are operating at once. In the laboratory, by contrast, the radiation source can be constant in intensity and position, known samples can be measured, and temperature and humidity can be controlled. Hence, both the performance of the instrument and the capability of the experimenter can be systematically evaluated. Steps to be taken to evaluate instrument performance in the laboratory are given below separately for the reflectance and emittance regions of the spectrum. Only after the instrument has been evaluated in the laboratory, and the experimenter can make repeatable and accurate measurements consistent with potential instrument performance in that setting, should one consider going into the field.

5.2.1 Reflectance Region

Linearity of Response. All modern instruments should have good linear response, although silicon photodiodes and InSb detectors are inherently more linear in their response than PbS and MCT detectors. An instrument is useless for most applications if, given a calibration of dark current and measurement of a white reference, intermediate reflectances between zero and 100% are not measured accurately. Part of this accuracy depends on the linear response of the instrument, but accuracy also depends on the degree to which the user thoroughly understands the instrument. For example, the white reference most commonly used is Spectralon®, a proprietary reflectance standard material manufactured by Labsphere, Inc. It is highly Lambertian, durable, and has a reflectance near 100% throughout most of the VNIR/SWIR. It is worth noting here, however, that the reflectance of this material is never quite 100%, and is not uniformly high at all wavelengths. The common assumption by unsophisticated users, that the reflectance of this material is constant at all wavelengths, can lead to subtle artifacts in an otherwise flat spectrum introduced by the reference instead of the target. Figure 5.1 shows a calibrated spectrum of a Spectralon® "white" reflectance standard supplied by Labsphere, which shows the discrete 6% absorption band near 2150 nm and falloff in reflectance to longer wavelengths common to all reflectance standards based on Halon. Such calibration curves supplied by Labsphere can be used to correct relative reflectance measurements to absolute reflectance. Naturally, an appropriate radiation source is needed to illuminate the white reference for linearity tests, as well as for the tests outlined below. While no source is going to have equal

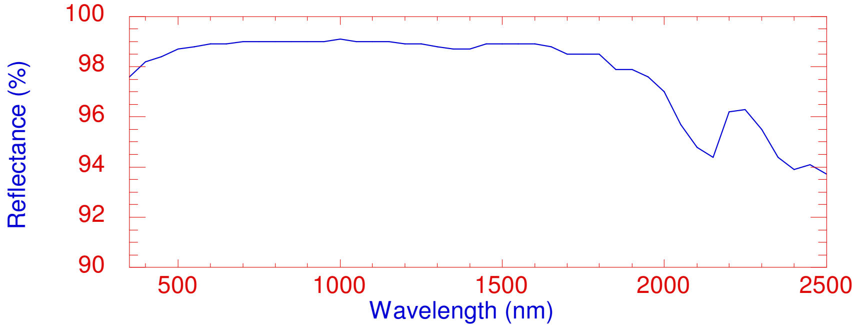

Figure 5.1. Absolute spectral reflectance of a Labsphere Spectralon® reflectance standard used as a 100% reference (Data from Labsphere calibration certificate No. SRS-99-010-5002-B).

intensity throughout the VNIR/SWIR, it is important to use a source that delivers sufficient energy at all wavelengths to provide an adequate signal-to-noise ratio. The normal tungsten filament incandescent sources are so deficient in the blue region of the spectrum that they should not be used. A quartz halogen lamp of sufficient power (~500 W) is recommended.

The linear response of an instrument can best be verified using a uniform source and calibrated lamps of different intensities (see discussion of radiometric calibration below). Access to such equipment is rare, and an adequate test of linearity can be made using any materials of known intermediate reflectance, but preferably materials with substantially Lambertian reflectance behavior, to avoid BRDF contributions to any measurement error. A selection of such materials can be generated by measurements of different samples using any properly calibrated laboratory spectrometer. Users without access to such a laboratory instrument may wish to purchase intermediate reflectance standards, such as the gray Spectralon® standards of varying reflectance available from Labsphere.

Wavelength Accuracy. Wavelength accuracy can be a problem with these instruments, even when new, but especially after any kind of shipment or rough field use (in the author's experience, shipping an instrument is equivalent to very rough field use, so instruments should be hand-carried to and from the field if at all possible). Most users check wavelength accuracy with samples displaying absorption bands that are sharp and at known wavelengths, sometimes supplied by the instrument manufacturer. Polyester cloth is a good example of a sample that is readily available, uniform in reflectance across a large area to accommodate different fields of view, easy to store or carry in the field, and possessed of sharp bands in the SWIR. Many minerals also display sharp bands in the SWIR, such as kaolinite and pyrophyllite.

Common materials with sharp bands in the VNIR are difficult to find. Low pressure arc lamps (Hg, Cd, Kr, etc.) can be used to generate discrete line spectra with a limited wavelength range. Sulfur and sulfide minerals display sharp absorption edges (as in the edge of a reflectance plateau) in the VNIR region. The exact wavelengths of absorption edges are, unfortunately, difficult to define because they are not perfectly vertical, and slopes vary slightly with particle size (Hunt et al., 1971). The derivative of the reflectance spectrum of a given sample for which the spectrum has been accurately measured with a laboratory spectrometer can, however, be used with success to check wavelength accuracy in the VNIR. Samples suggested and the approximate wavelengths of their respective absorption edges are: pure sulfur (450 nm), realgar (550 nm), cinnabar (600 nm), and stibnite (780 nm). The absorption edges are steepest for the finest particle sizes of these minerals. These and other mineral samples can be purchased from mineral supply houses, such as Ward's Natural Science Establishment, Inc. of Rochester, NY (www.wardsci.com).

Minerals having discrete and very sharp bands in the VNIR are rare earth oxides, but they are, as the name suggests, difficult to acquire in bulk. Labsphere imbeds small amounts of rare earth oxides in Spectralon® to make wavelength calibration standards. Of these, their holmium oxide standard has bands extending from the VNIR well into the SWIR, and can thus be used to calibrate the entire wavelength range.

Field of View. As pointed out in the Instrument Description sections above, instrument fields of view may be larger than their angular size would suggest, and different detectors may view somewhat different fields of view. Further, aiming devices may not be boresighted with the spectrometer. A pinhole radiation source can be used to map out the FOV at different wavelengths and verify boresighting, commonly by moving the pinhole in front of a fixed instrument with a grid underneath on which to map out instrument response. If it is difficult to obtain a pinhole source of sufficient intensity, a less exact map of the FOV can be made by moving a brightly-illuminated white reference panel slowly into the field from top, bottom, and all sides.

A field of view typically does not have a sharp cutoff, but rather an asymptotic approach to zero throughput. Thus, the measured field is often smaller than the true one. Consequently, once the field of view of the instrument has been measured, it is recommended that, if possible, this field be overfilled by a factor of two during spectral measurements, to avoid spectral contamination by adjacent materials. Adjacency effects due to atmospheric scattering, however, are not a significant factor at the short distances normal for field measurements.

Instrumental Artifacts. Instrumental artifacts may occur in spectra, such as intensity offsets or excessive noise at wavelengths of detector changes, or excess signal at some wavelengths due to stray radiation problems (a common problem, and one difficult to diagnose without careful, quantitative measurements). Identification of such artifacts can usually be accomplished by measurement of targets with known reflectance spectra. In this case, a material with a very flat spectrum is preferred, so that the artifacts, if any, are prominently displayed. A relatively bright target will usually emphasize intensity offsets or noise spikes, while excessive brightness of a relatively dark target can be used to identify stray radiation. Calibrated gray Spectralon® reflectance standards (e.g., an 80% and a 2%) work well, but any known material will do. Dave Kelch of MTL Systems suggests that a still better way to identify the presence of stray radiation is to use cutoff filters in front of the source. Wavelengths of these filters should be chosen to bracket wavelengths of order-sorting filter or grating changes to test specifically for high order leakage of shorter wavelength radiation, in addition to the presence of light physically scattered within the instrument.

Environmental Tolerance. The tolerance of a field instrument for environmental extremes, particularly of heat and cold, is something to verify before going into the field. It is usually easy to find a sauna in which to test the entire system for heat tolerance. If a walk-in refrigerator is not available for a cold tolerance test of the entire system, individual components, especially the computer, can be tested in a residential refrigerator. The computer should also be tested in bright sunlight to assure that the screen is readable under those conditions.

Figure 5.2. Brett Sink of MTL Systems calibrates their GER Mark IV using a portable uniform calibration source built by MTL. The extremely rugged control box of the Mark IV (resting under his right hand) is replaced by a laptop computer for the Mark V version of this instrument.

Radiometric Accuracy. Not all users will be interested in absolute radiometry. Those who are will want to calibrate instrument response as a function of instrument (and especially detector) temperature. This is not a trivial exercise, requiring a uniform source of radiation of known intensity as a function of wavelength. Such a uniform source basically consists of an integrating sphere, a calibrated (traceable to NIST) source of radiation to the interior of the sphere, and a regulated power supply to operate the radiation source. The interested reader is referred to the NIST Web site (www.nist.gov) and local NIST laboratories for more information on calibration and uniform sources. The recent report by Goetz et al. (1998) suggests how difficult it is to assure absolute accuracy of such sources.

If highly accurate (1%) measurements are desired in the field, a portable uniform calibration source is needed, such as that shown in Figure 5.2. While laboratory calibration sources are readily available, a portable version would need to be custom made. MTL Systems constructed their own portable source, and Dave Kelch of MTL can be contacted for more information at dkelch@mtl.com. Labsphere, which supplies free brochures describing uniform sources and calibration techniques, can also be contacted for more information (contact Art Springsteen, the Principal Scientist at Labsphere, at art_spring@labsphere.com).

Users who are interested in measuring radiance, but unable to gain access to a calibrated uniform source, can at least find out if they have a problem by using any light source on a regulated power supply and a white reference. A hair dryer can provide thermal stress to the spectrometer. With a constant light source, and a fixed geometry, any difference in spectral radiance over time indicates a problem.

5.2.2 Emittance Region

Radiometric Accuracy. While radiometric accuracy may be of little consequence for the common relative reflectance applications in the reflectance region, it is crucial for all applications in the thermal emittance region. Thus, the first test of instrument performance in this region should be one for radiometric accuracy. This test is accomplished by determining the accuracy with which measurements of black bodies recover a Planck function (the shape of the spectral curve) representing the correct blackbody temperatures (see Figure 4.4 and associated text in Section 4.2.2). Simple in concept, this test can be difficult to carry out because it demands both use of a relatively large aperture blackbody that is truly "black," and precise knowledge of its temperature. Outside of large and well-equipped optics laboratories, these two demands are not easily met.

With regard to the blackbody, the interior of any 15° cone is "black," not because of any interior coating, but because the multiple internal reflections of emitted photons engendered by its shape result in a Planckian distribution of escaping infrared radiation. When a large exit aperture is needed, the 15° cone shape of the classic "perfect" blackbody results in a very large object indeed, which is difficult to keep at a uniform temperature. Most laboratories use a blackbody simulator, which achieves the result without the bulk, by using a cavity of smaller size (larger solid angle) coated with a highly absorbing paint. Absorption by the paint substitutes in part for multiple internal reflections. Paints that look quite black in the visible, however, often are not black in the thermal infrared, making such blackbody simulators difficult to make. Yet, the importance of such equipment is enhanced by the need for good portable blackbody simulators for instrument calibration in the field. No matter how well an instrument performs in the laboratory, its ultimate performance in the field is limited by the accuracy of this calibration.

One solution commonly applied to field blackbodies is to use a flat plate that has been grooved like a phonograph record with v-shaped grooves. These grooves act as small cavities, but the performance of such blackbodies is strongly controlled by the absorption qualities of the paint. Usually, a paint with a velvet-like surface is used, so that the paint itself provides microscopic cavities to amplify the effect of its absorbing pigments. The emissivity of the flat plate of one such blackbody is shown in Figure 5.3, demonstrating that this technology can produce an excellent blackbody simulator, even without the additional internal reflections allowed by whatever cavity lies above the flat plate surface. However, the less than perfect blackbody behavior is a source of error, as discussed and quantified in Korb et al. (1996). A second source of error is the uncertainty with which the actual temperature of the blackbody is known. Blackbody temperatures are usually measured with platinum resistive thermometers

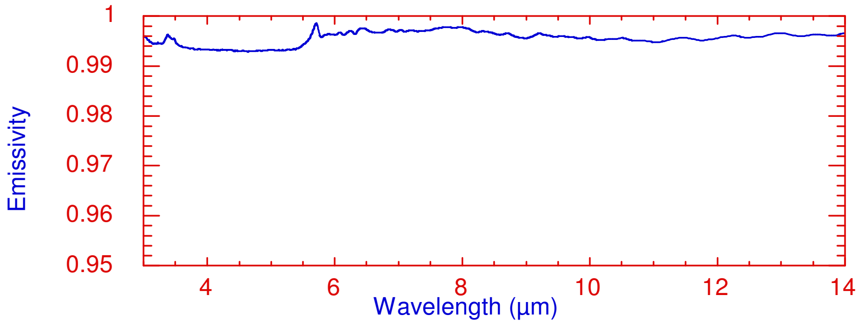

Figure 5.3. Emissivity of the plate of a flat plate blackbody calculated from its directional hemispherical reflectance using Kirchhoff's Law. Black paint was applied by GER to a field blackbody supplied by Designs and Prototypes. (Figure from Korb et al., 1996; measurement by John Salisbury using a Nicolet System 510 with calibrated integrating sphere.)

traceable to NIST embedded in the body of the blackbody. Temperature stability of the blackbody and measurement accuracy of the thermometer together typically result in an error of at least ±0.1° C.

Within the limits imposed by the emissivity of the blackbody used and the accuracy of its temperature measurement, one can measure the performance of the field spectrometer in recovering both shape and magnitude of blackbody emittance.

Linearity of Response. Linearity of response was introduced above in Sections 4.2.2 and 4.3.2 in describing the performance of different instruments. Two kinds of error can be distinguished. First, is the interpolation error that occurs when the temperature of a blackbody at a temperature intermediate between the calibration temperatures is not accurately recovered from measurements of emittance. A common strategy is to make calibration measurements close together in temperature to minimize interpolation error between them, but this is a mistaken approach when instrument response is highly linear (which is true for the two instruments reviewed above). Thus, the farther apart the calibration temperatures are, the more precisely can be determined the slope of the calibration curve, and the greater the accuracy of blackbody temperature retrieval. In practice, a temperature interval of about 30° C is recommended for instrument calibration (Korb et al., 1996).

Extrapolation error for measurements of temperatures beyond the limits of the calibration temperatures is common when measuring very cold targets (see Figures 4.5 and 4.9, and associated text). Measurement of a polished aluminum target submerged in liquid nitrogen is a good way to test extrapolation error. Keeping the foreoptics of the instrument below the rim of the dewar during measurement will minimize atmospheric emission lines in the data by placing the foreoptics in a nitrogen atmosphere (compare Figures 4.5 and 4.9).

Wavelength Accuracy. The typical FTIR instrument has very high wavelength accuracy, due to the excellent frequency stability of the gas laser typically used for a frequency reference. The microFTIR, however, must pay for the compact nature of its refractive optics and laser diode with the potential for wavelength inaccuracy. The imperfectly-known, wavelength-dependent refractive index of the KBr optics, and the tendency of laser diodes to shift frequency with changing temperature, both can contribute to such error. Thus, a wavelength check, and sometimes correction, is necessary. One wavelength standard commonly used is polystyrene film in transmittance, but it has few bands in the MWIR. The use of polyester cloth in transmission or emission is one recommendation made here, because it has many sharp bands in both the MWIR and LWIR, as shown in Figure 5.4. A source of still sharper bands is the atmosphere, water vapor bands of which were used by Hook and Kahle (1996) to calibrate the JPL microFTIR. Andrew Korb, SAIC, has a collection of atmospheric spectra recorded at very high spectral resolution and accuracy that he has deconvolved (resampled at lower spectral resolution) to a resolution similar to that obtained with the microFTIR and used for calibration of this instrument (Korb and D'Aria, 1998). These spectral data can be obtained from Andrew via e-mail (korba@erols.com).

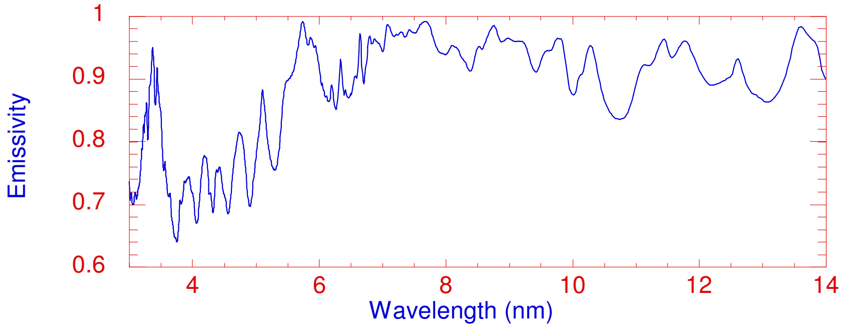

Figure 5.4. Emissivity of polyester cloth calculated from its directional hemispherical reflectance using Kirchhoff's Law.

The X-axis in Figure 5.4 is shown in wavelength, but any wavelength corrections should be made in frequency space (wavenumbers), since any correction is more likely to be linear in wavenumbers, the units in which FTIR instruments operate.

Field of View. The same FOV considerations pointed out for the reflectance region of the spectrum hold for the emittance region. Instead of a pinhole light source, a soldering gun with a small soldering tip is recommended for mapping out the field of view in the thermal infrared, although care must be taken not to saturate the detector. If necessary, the soldering gun can be used with a variable power supply.

Instrumental Artifacts. Blackbody targets serve the purpose of identifying instrumental artifacts in the emittance region. Sometimes these artifacts can be subtle and difficult to diagnose. One instrumental artifact that is unique to FTIR instruments occurs when electrical noise of a given frequency is superimposed on the detector output. Any such electrical noise is deconvolved during the Fourier transform into an apparent optical signal. Two common sources of such noise are vibration and electrical pickup. The JPL microFTIR experienced an example of a vibration problem due to its temperature-controlled blackbody. Heat is extracted from this blackbody by a small fan which, at one point, lost a fan blade. The imbalance in the shaft resulted in vibration, which was transmitted to the slightly microphonic detector during calibration, when the blackbody was snugly fitted over the foreoptics. The resulting range of electrical frequencies deconvolved into a burst of noise superimposed on the spectrum near 11 µm.

Under normal field or laboratory conditions electrical pickup is not a problem, but our Johns Hopkins University microFTIR did experience this when operated near a high powered radar installation on a military reservation. The key to recognizing electrical pickup is that the typical narrowness of the frequency superimposed on the detector output results in a very narrow spike of apparent energy in the optical spectrum.

Environmental Tolerance. The same considerations and approaches apply to emittance instruments as to instruments used in reflectance (see above).

End-to-End Calibration. Ultimately, most users of emittance spectrometers wish to determine emissivity. Thus, a successful measurement of emissivity is the bottom line of both instrument performance and user capability. As explained in more detail in Section 5.5.2 on data reduction and analysis, one must estimate target temperature to infer emissivity. Assuming that some form of software is available to assist in this critical step (see Section 5.5.2), or that the target temperature is measured manually, then the user should be able to reliably retrieve the emissivity of a known target that is not a blackbody. In fact, a target quite far from a blackbody should be selected in order to test the accuracy of subtraction of reflected downwelling radiance by the algorithm being used to calculate emissivity. We often use a quartz sand (size range 75-250 µm, washed clean of clinging fines) for such measurements.

Figure 5.5 shows the kind of repeatable results with a test sample that one should be able to achieve in the laboratory. Although signal-to-noise declines beyond 12 µm because of declining detector sensitivity, the greater divergence of the calculated emissivities at longer wavelength is due primarily to slight errors in estimating the temperature of the quartz sand using Korb and D'Aria's (1998) algorithm described in Section 5.5.2 below. A slight temperature error imparts a tilt to the overall emissivity curve, which becomes more obvious at longer wavelengths.

The absolute accuracy of such measurements is determined by comparison with directional hemispherical spectra of the same sample and exercise of Kirchhoff's Law. An average of several laboratory measurements should be within ±1% of absolute emissivity calculated in this manner.

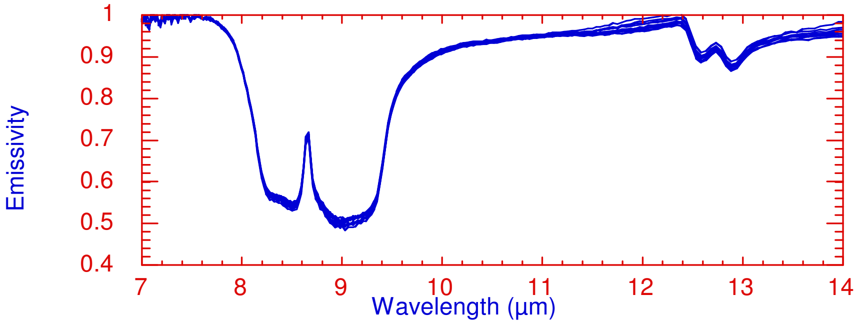

Figure 5.5. Emissivity of quartz sand measured and calculated twelve times under laboratory conditions, with the sand heated by a hot plate to approximately 52° C (from Korb et al., 1998).

If accurate and repeatable measurements of spectral emissivity cannot be made in the laboratory, then it is useless to go into the field, because the laboratory environment provides four significant advantages over field measurements. First, the sample can be made as hot as desired to improve signal-to-noise (note that the sample must be hotter than the ceiling and walls, or downwelling radiance will equal sample radiance, resulting in a blackbody). Second, the downwelling radiance from ceiling and walls is constant and takes the form of a smooth curve close to a Planck function, without the sharp atmospheric emission bands that are so difficult to correctly subtract from target emission in field measurements. Third, the diffuse gold plate or other material used to measure downwelling radiance is at approximately the same temperature as the ceiling and walls, making it unnecessary to account for self-emission from the gold plate in calculating downwelling radiance. Finally, instrument temperature tends to remain constant in the benign laboratory environment, making calibration of instrument self-emission relatively easy.

5.3 Data Collection - Recognizing Environmental Effects

5.3.1 Reflectance Region

As pointed out in Section 5.1, field measurements to support calibration/validation of overhead sensors should be made at the time of overflight if possible, so that the effects of sun angle and atmospheric absorption will be fully represented in the field data. However, in planning such a data collection, environmental effects must be kept in mind, together with the desired level of accuracy required by the specific application. For example, if high accuracy is required in measurement of upwelling spectral radiance from different scene elements, spatial and topographic variations in water vapor within a scene demand multiple measurements (see Section 2.1.2). Temporal variations in water vapor demand that these measurements all be made simultaneously, or very nearly so, with overflight. Obviously, this cannot be accomplished with a single field spectrometer, but simultaneous measurements in every pixel of a scene of any size are also obviously impractical. Desired accuracy must be traded off against cost and practicality. Usually, calibration/validation efforts are focused on one or two scene elements, preferably ones close together spatially and topographically. Manmade calibration panels are commonly used, both because they test the complete range of system response, and because they can be made large enough to provide "pure" pixels (pixels, the radiance of which is not contaminated by adjacency or edge effects).

Highly accurate (1%) radiance measurements require field calibration with a uniform source, although laboratory calibrations at different temperatures can be used in conjunction with field measurements of detector temperatures.

If relative spectral reflectance is the desired measurement, then environmental effects suggest that the most accurate and spectrally complete measurements can best be made under clear sky conditions within two hours either side of solar noon, and at a season when the sun is high in the sky (see Figures 2.2 and 2.3 in Section 2.1.2). In this way, the signal-to-noise ratio is maximized, and atmospheric variability and obscuration of spectral data by water vapor absorption bands is minimized. This recommendation to start measurements late and quit early means that data collection must be carefully planned to cover the maximum number of targets. Typically, enough targets can be measured in four hours to more than fill the remaining hours of any day with data reduction chores.

A well-characterized, known sample should be carried into the field and its reflectance measured occasionally to provide a check on instrument performance. The white reference shoud be measured as a target every five minutes or so, even under ideal conditions. If the resulting spectrum is not a flat 100% line, then instrument responsivity and/or solar irradiance have changed, and a new reference must be stored. The most common mistake in spectral field measurements is to fail to store a fresh reference on a timely basis.

Sometimes operational constraints require measurements under less than ideal conditions, with low sun angle or cloudy skies, or both. In such cases, there is a premium on rapid measurement of both target and reference to compensate for irradiance variability. This puts a premium on a fast instrument, and the number of scans averaged should be reduced to the minimum practical number to speed up the measurement process still more. Under such conditions, use of active light sources, or a double beam instrument like the GER Mark IV, and/or an active instrument like the PIMA II, should be considered.

5.3.2 Emittance Region

When emittance measurements are made to support sensor calibration/validation, environmental effects are similar to those describe above for reflectance. Upwelling spectral radiance measured from different scene elements depends critically on the amount of reflected downwelling radiance, as well as target temperature and emissivity. Target temperature changes with solar zenith angle and cloud cover, while atmospheric downwelling radiance changes dramatically with changing water vapor content, cloud height and distribution, and atmospheric temperature. Again, these effects, and the spatial, topographic, and temporal variations in them, demand field measurements simultaneous with sensor overflight for calibration/validation applications. As in the case of reflectance measurements, manmade panels of known emissivity are often used when sensor field of view is not too large to make this impractical.

Where measurement of spectral emissivity of targets is the purpose of the field exercise, there is a relatively long time period during which good data can be obtained, at least under ideal measurement conditions. Such conditions (a clear, dry and stable atmosphere) minimize the amount and temporal variability of downwelling radiance. Under these conditions, maximum contrast between target radiance and downwelling background radiance (hot target, cold atmosphere) will yield the best data. Unlike the case of relative reflectance measurements, this condition is not necessarily met near solar noon, however, because the atmosphere typically warms along with the target as the sun rises. Further, cloud cover and atmospheric instability and variability are often made worse by the effects of rising thermal currents in the atmosphere during the hottest portions of the day. Thus, good data can often be obtained early in the morning or late in the afternoon, as long as the target is warm enough to provide both a good signal-to-noise ratio and good thermal contrast with atmospheric emission.

As in the case of reflectance, under less than ideal conditions there is a premium on rapid measurement of target radiance and downwelling radiance before conditions change. One way to speed up measurements is to trade off spectral resolution (consistent with the goal of the application) for less signal integration time. Molecular vibration bands of liquids and solids are sufficiently broad that 8 wavenumber resolution is perfectly adequate for most applications. If the resolution of the Bomem is changed from 1 wavenumber to 8 wavenumbers, the same signal-to-noise ratio can be obtained with one eighth the measurement time. The microFTIR resolution, however, is fixed and cannot be changed.

Even without a reduction in spectral resolution, it is advisable to reduce the number of scans by a factor of two or more under adverse conditions. Decreasing the number of scans by a factor of two only increases the noise by the square root of two. The noise contributed by inadequate extraction of downwelling radiance, under adverse conditions, where downwelling radiance changes faster than the time required to measure both sample radiance and downwelling radiance, may easily exceed the noise introduced by limiting integration time (see Figure 5.6). Whatever the strategy used to speed up the process, it is essential to measure sample radiance and downwelling radiance

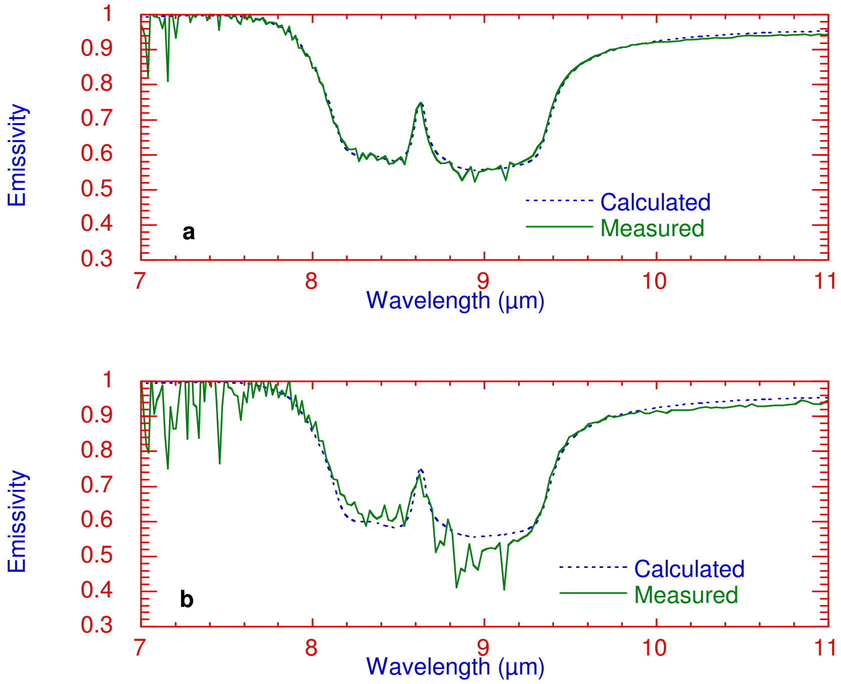

Figure 5.6. Comparison of emissivity calculated from directional hemispherical reflectance with emissivity derived from field measurements (a) under stable atmospheric conditions with low water vapor content, and (b) under unstable atmospheric conditions with high water vapor content. Scan time for target and reflector of downwelling radiance in both cases was 16 seconds. Obviously, downwelling radiance changed faster than the measurement process under adverse conditions as in (b), as shown by the water vapor emission bands incompletely extracted from the sample emissivity. This is a quartz sample with a different

particle size, and hence a different emissivity, compared to that measured for Figure 5.5. (Data from Korb et al., 1996.)

sequentially, and as close together in time as possible. Figure 5.6 shows the importance of measuring the downwelling radiance rapidly, but it must also be measured correctly. Direct measurements of downwelling radiance at different upward-looking angles, followed by an averaging process, take too much time under most observing conditions. That is, atmospheric condtions will change before the measurement process is complete. Thus, downwelling radiance is usually measured using a highly reflecting diffuse surface. The diffuse nature of such a surface allows total hemispherical downwelling radiance to be recorded with a single measurement. A highly reflecting (very low emissivity) material minimizes the amount of sef-emission from the diffuse surface which must be subtracted from the apparent downwelling radiance.

A diffuse gold surface (Infragold®) generated on an alumimum substrate by Labsphere is often used for downwelling radiance measurements. It has a reflectance typically of 94-96%, with absolute calibration available from Labsphere. Unlike Spectralon®, however, the BRDF of Infragold® is not highly diffuse, but is sufficiently so to provide excellent results. The drawbacks to Infragold® are that large surfaces are heavy, can be contaminated quickly by windblown dust, and are expensive.

An inexpensive substitute especially suitable for field use is heavy duty aluminum foil. The bright side of <u>fresh</u> foil has the theoretical reflectance of aluminum (97%). It can be crinkled several times in different directions and then smoothed out to provide a quasi-diffuse surface with a reflectance of about 94%. Taped to cardboard, this provides a light weight reflectance surface that can easily be renewed if contaminated by blowing dust. As pointed out in Section 2.2.5, however, one disadvantage of using foil is that its temperature can vary quickly with wind speed because of its relatively low thermal inertia.

As pointed out in Sections 4.2.2 and 4.3.2, calibration extrapolation error can result in downwelling radiance measurement anomalies when the atmosphere is extremely clear and dry, resulting in a very cold sky. Instrument response, calibrated at ambient temperature, is not sufficiently linear to accurately measure downwelling radiance under such conditions. One solution is to use a reflecting surface with relatively low reflectance and high emissivity. In this case, self-emission from the surface can bring the total radiance measured into the calibration range, if the reflectance plate is heated by the sun or any other heat source. We have used a flame-sprayed brass coating on an aluminum substrate provided by Labsphere with success for this purpose. With an emissivity of about 0.25, this material has much greater self-emission than the highly reflecting surfaces described above, with emissivities ranging from 0.04 to 0.06. The disadvantages of flame-sprayed brass are its cost, its tendency to tarnish, and the need to measure its temperature quite precisely to account for its self-emission in determining the magnitude of downwelling radiance. With the low emissivity materials, on the other hand, errors in estimating their temperatures have relatively little effect on downwelling radiance calculations. In a pinch, if these materials are kept in the shade between measurements, they can be assumed to be at air temperature.

Under both good and bad atmospheric conditions, it is highly recommended that a known sample be periodically measured to verify that the instrument is working properly, and so that estimates can be made of the accuracy of derived emissivities under the particular conditions of measurement. We have often used quartz sand for this purpose, but Simon Hook of JPL recommends the use of silicon carbide as a test sample. Because of its use as a grinding medium, specific particle sizes of this material are easy to obtain, and their spectral emissivity should be highly reproducible in the laboratory. More important for use of a test sample in the field, the reststrahlen bands of silicon carbide fall in the 10-12 µm region where extrapolation error is greatest for the microFTIR. Thus, this material can be used to test whether or not the sky temperature is so cold that extrapolation error is occurring.

5.4 Record Keeping

Record-keeping requirements are the same for both regions of the spectrum, the principal requirement being to record whatever data would be needed to make the spectral measurements useful to someone else. This is a good criterion to use, even if the spectra will never be used by others, because memory inevitably fades.

Extremely detailed record-keeping is recommended in the HYMSMO Program Ground Truth Protocol (HYMSMO Program Office, 1997), with separate field logs for spectral measurements, photography, and environmental data. Perhaps the most valuable kind of documentation is photographic, with each photograph worth the proverbial thousand words. A photograph of the target is essential, preferably with the field spectrometer in the field of view, both for scale and to document the instrumentation used and its orientation. An all-sky photograph will show both extent and location of cloud cover, as well as solar altitude and azimuth. Camera backs that automatically record date and time are recommended.

With regard to text, the log forms recommended by the HYMSMO Program Office (1997) are excellent, but assume a larger operation, with more environmental information (such as radiosonde, sun photometer, and pyranometer data) than is typically part of a field measurement. These logs may be shortened or combined by other experimenters for other applications, as long as the following basic data are systematically provided. WHO made the measurements? WHAT was measured? WHEN were the measurements made? WHERE was the target located? HOW were the measurements made? WHY were the measurements made?

Digital spectral data, photographs, and other data should, of course, be keyed to the field log, preferably by means of their file names. The HYMSMO Program Office (1997) recommends a file name convention for digital spectral data having the format:

ddmmmyyR.nnn

where dd is a two digit number indicating the day of the month, mmm is a three character code for the month, yy is a two digit number indicating the year, R indicates that this file is a reduced spectral data file, and nnn is the sequence number for the file collected on the given date by a given instrument.

If this convention were used for other data, such as photographic data, the "R" character could be changed to a "P." By using such substitutes for the R character, all data types could be linked together and to the field log. Longer file names available with newer operating systems provide more flexibility to this approach.

5.5 Data Reduction - Making Raw Data Useful

5.5.1 Reflectance Region

Data reduction always takes longer than anticipated, at least if truly useful data are desired. Even in the reflectance region, where the spectrometer operating program usually produces reduced data in the form of radiance or relative reflectance in near-real time, each digital record needs to be individually examined to detect and delete those spectra with unacceptable instrumental or atmospheric artifacts. In addition, if absolute reflectance is a goal, then relative reflectance data must be corrected by multiplying the spectrum by the reference material calibration curve (e.g., Figure 5.1). Radiance measurements may also need to be corrected for the effects of temperature on instrument responsivity.

5.5.2 Emittance Region

In the emittance region, the most straight forward measurement is total upwelling radiance (target self-emission plus reflected downwelling radiance). All this requires is measurement of two blackbodies at different temperatures for calibration, and then a measurement of the target. Figure 5.7 shows such a measurement of a quartz sand test sample (curve b).

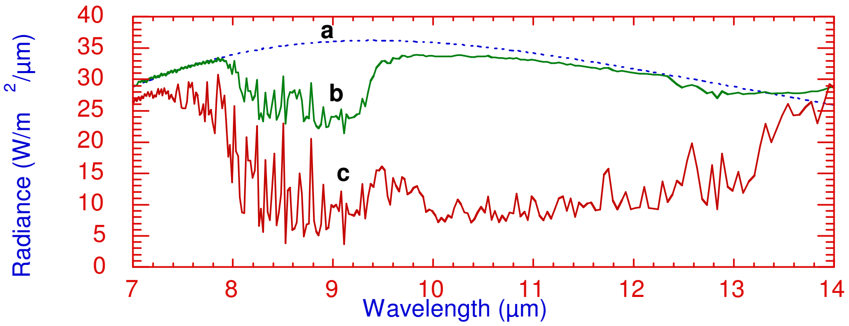

Figure 5.7 (a) calculated spectral radiance of a blackbody at 35.82°C, (b) measured total upwelling radiance from a quartz sand, and (c) measured downwelling radiance. Measurements made with the microFTIR by Andrew Korb, SAIC, at Yuma, AZ on October 18, 1995.

If calculation of spectral emissivity is the goal, then measurements become more complex and data reduction can be a difficult process. It is not the purpose of this report to recapitulate that process in detail (interested readers are referred to Hook and Kahle, 1996; and Korb et al., 1996), but a brief summary will show the value of several recently written algorithms that are extremely useful in this process.

The first problem in calculating spectral emissivity is that total upwelling target radiance is composed of both target emittance and reflected downwelling radiance. Consequently, as described above for data collection, a second measurement is made of downwelling radiance, usually as it is reflected from a quasi-diffuse, highly reflecting surface, so as to determine hemispherical downwelling radiance. For field measurements, the temperature of this reflecting surface should be measured, and its emissivity known, so as to subtract its emission from the reflected downwelling radiance (this self-emission becomes an important factor when using a relatively low reflectance material like flame-sprayed brass to avoid extrapolation error, as described in Section 5.3.2). Figure 5.7 shows the measurement of downwelling radiance (curve c) made immediately after the measurement of quartz sand radiance. A flame-sprayed brass plate was used to measure downwelling radiance because of the extremely cold sky temperature at this desert site in October under very clear sky conditions. Temperature of the brass plate (54° C) was measured with a thermocouple.

Ignoring for the moment reflected downwelling radiance, the target radiance due to self emission alone is a function of both temperature and emissivity. The reader will recall that emissivity is basically the efficiency with which a material emits infrared radiation. A blackbody has the highest theoretical radiation efficiency (designated 1.0), and the emissivities of all materials are determined by how closely they achieve this theoretical efficiency. Bare aluminum, for example, has a very high reflectance and a correspondingly low emissivity (~0.03 for a completely smooth surface). Thus, even a relatively hot aluminum surface is such an inefficient radiator that its radiance would be equivalent to that of a blackbody well below zero. When the emissivity of a material changes with wavelength due to the presence of molecular vibration bands, an emissivity spectrum results that can be used to determine composition. What this changing emissivity means, however, is that at any given wavelength one cannot tell how much of the radiance is due to temperature, and how much is due to the efficiency of radiation. Only if the temperature is known, can the emissivity be calculated by comparison with the radiance expected from a blackbody at that temperature. This is the crux of the emissivity calculation problem.

The temperatures of some targets, such as bare metals, are relatively simple to measure directly with thermocouples. These targets are usually manmade, with smooth surfaces for good thermal contact of the sensor, and high thermal conductivity, so that the sensor does not significantly change the surface temperature. Many target materials do not meet these criteria, and their temperatures must be estimated in some way. Target temperature estimation error is a major source (often <u>the</u> major source) of error in emissivity calculations (Horton et al., 1998).

The classic method of estimating temperature is to assume that target emissivity approaches that of a blackbody at some wavelength in the measurement range (e.g., Murcray et al., 1970; Kahle and Alley, 1992). Then the maximum brightness temperature derived from target radiance as a function of wavelength is assumed to be the target kinetic temperature This unit emissivity method applied to the quartz radiance in Figure 5.7 results in a temperature estimate for the quartz of 35.82° C (note here that the blackbody spectral curve (a) was not fitted to the quartz radiance spectrum in the wavelength region beyond 13.5 µm, because a low signal-to-noise ratio for the radiance measurement beyond 13.5 µm made the data unreliable).

More sophisticated algorithms are now available that allow assumption of less than unit emissivity (called the "maximum emissivity" method), and fit target radiance to a Planck function (blackbody spectral curve) for any emissivity over any spectral range with great success. Korb and D'Aria (1998), for example, have developed software that works on either DOS-based or Macintosh computers (for more information, contact Andrew Korb at korba@erols.com). Using this software, and assuming a maximum emissivity of 0.996 for the quartz at the wavelength of maximum brightness temperature, the temperature estimate of the quartz sand measured for Figure 5.7 was refined only slightly to 35.84° C. If the maximum emissivity were further from 1.0, the difference in estimated sample temperature would, of course, be greater.

In the case of the quartz sample measured for Figure 5.7, the maximum emissivity was known from measurement of directional hemispherical reflectance. For an unknown sample, the maximum emissivity approach can obviously lead to error if the assumed maximum emissivity is incorrect. For most natural materials, the assumption of a maximum emissivity near 1.0 is a good one in the 8-14 µm atmospheric window (Salisbury and D'Aria, 1992). Carbonates, however, do not follow this rule, having maximum emissivities near 0.95 in this wavelength region, while manmade materials like bare metals have much lower emissivities. To use the maximum emissivity method, it is only necessary to know the average emissivity of different classes of materials to derive a fairly good temperature estimate. This is best accomplished in the 8-14 µm region, where emissivities tend to be considerably higher than in the 3-5 µm region (Salisbury and D'Aria, 1994).

Simon Hook at JPL has developed an IDL-based program package called FESTER (Field Emission Spectrometer Tool for Emissivity Retrieval), which allows adjustment of different data input parameters, and contains a variety of methods for recovering sample temperature (information on this program package can be obtained from Simon Hook at simon.j.hook@jpl.nasa.gov). These methods include the maximum emissivity approach outlined above, and an interesting differential atmospheric line method first proposed by Smith et al. (1996).

The differential atmospheric line method varies sample temperature to minimize the residual atmospheric emission lines that should be removed in a proper correction for reflected downwelling radinance. As shown in Figure 5.8, calculation of apparent emissivity without extraction of reflected downwelling radiance results in a spectrum in which atmospheric emission lines from the downwelling radiance are superimposed on the quartz reststrahlen bands where they are preferentially reflected.

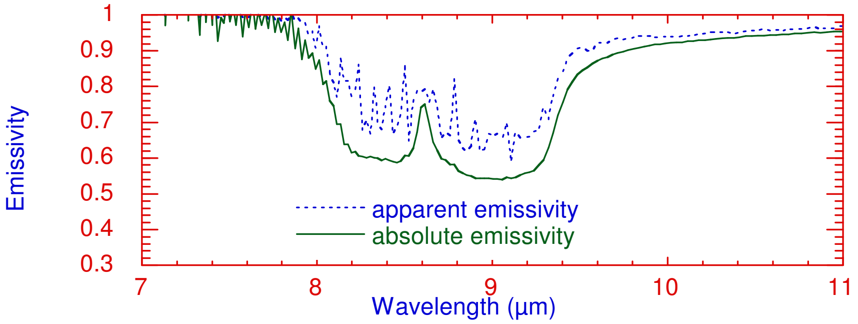

Figure 5.8 Apparent emissivity calculated by ratioing the quartz radiance curve in Figure 5.7 against a 35.84° C Planck function, without subtracting reflected downwelling radiance, compared to absolute emissivity calculated with reflected downwelling radiance removed. Measurements by Andrew Korb, as above for Figure 5.6.

This figure illustrates how subtraction of the reflected downwelling radiance essentially eliminates the water vapor emission lines from the spectrum, and deepens the reststrahlen bands.

The differential atmospheric line method takes advantage of the downwelling radiance subtraction process to refine the estimate of target temperature. When the sample temperature estimate is too high, subtraction of the downwelling radiance results in negative spikes superimposed on the emissivity spectrum due to atmospheric emission lines. When the sample temperature estimate is too low, the atmospheric emission lines are seen as positive spikes. By iteratively changing the sample temperature estimate to minimize the atmospheric lines, the correct sample temperature can be established. For this approach to work, however, one must assume that the measurement of downwelling radiance is correct. That is, that the instrument has worked properly and that the downwelling radiance did not change between the time the target was measured and the downwelling radiance was measured. It appears that this approach was developed independently at the University of Hawaii by Horton et al. (1998), and more information on their approach can be obtained from Keith Horton at kieth@kahana.pgd.hawaii.edu.

5.6 Data Analysis

Data analysis is extremely time-consuming when done properly, and is probably the most underfunded aspect of hyperspectral remote sensing today. Millions are spent for data acquisition and pennies for analysis. The literature, gray and otherwise, is replete with "Preliminary Reports", but sadly lacking in exhaustive studies. One problem is that a preliminary analysis of the data is usually rewarding in a superficial way. Known targets in a scene can be used for in-scene calibration of both atmospheric effects and sensor response. Then these and similar targets in the scene can be discriminated from background, and thresholding and color coding can make it appear that target detection is sure and certain. This is, however, a far cry from the ultimate goal of hyperspectral remote sensing, which is identification of unknown targets in a scene, without a known ground calibration source, usually by searching a spectral library.

AVIRIS investigators have made some progress toward this goal by working on methods for pixel-by-pixel atmospheric correction of hyperspectral data in the reflectance region using the spectral data themselves (Green, 1991; Green et al., 1991). Corrected airborne spectral data have been used successfully for compositional mapping of surface materials using various spectral matching algorithms and a spectral library of mineral and rock spectra (e.g., Rowan et al., 1995).

Likewise, NASA investigators on the ASTER Science Team have made progress in separating temperature and emissivity in remotely sensed multispectral LWIR data (see Web site asterweb.jpl.nasa.gov). At the same time, they have assembled a spectral library of mineral, rock, soil, vegetation, snow and ice spectra for comparison with remote sensing data from 0.4 to 14 µm (see Web site asterweb.jpl.nasa.gov/speclib; see also the U. S. Geological Survey spectral library at web site speclab.cr.usgs.gov).

Exhaustive data analysis is expensive and time consuming. But, it is only by such means that sensors are thoroughly understood, and the ultimate potential of hyperspectral remote sensing can be determined. This means that overhead sensor performance and atmospheric extraction algorithms must be improved until the spectral reflectance and emissivity of surface materials can be accurately extracted from the remote sensing data. In the initial stages of sensor development, this is better achieved by repeated measurements of the same one or two sites, so that hardware and software can be perfected, rather than by seemingly more productive measurements of multiple sites. Overhead data collections need not only to be accompanied by field measurements, but also need to be followed up by additional field measurements to help explain the inevitable anomalous results turned up by initial data analysis. Spectral libraries need to be fully populated, and spectral search algorithms tested and re-tested as observational data improves. Until data analysis receives the same level of support as data acquisition, the promise of hyperspectral remote sensing will not be realized.

6.0 ACKNOWLEDGMENTS

Many colleagues helped make this report possible. Tim Bowers of the Earth Satellite Corporation ably assisted the author by making field measurements under a variety of conditions to illustrate environmental effects. Jim Crowley of the U. S. Geological Survey was especially helpful, lending the use of field instruments, giving instruction in their use, and making many supporting measurements in the field and laboratory. Ponder Henley of the U. S. Army Corps of Engineers Topographic and Engineering Laboratory was also extremely helpful, sharing his experience and making numerous measurements with the GER 3700, some more than once, for which the author is profoundly grateful. Dave Kelch of MTL Systems made measurements of kaolinite and polyester with a GER Mark IV, and gave freely of his time and experience. Much useful information, and measurement data were contributed by manufacturers' representatives, especially Tom Corl of GER, Phoebe Hauff and Chris Endler of Spectral International, Peter Dybwad and Win Wadsworth of Designs and Prototypes, and Dave Beal and Alex Goetz of Analytical Spectral Devices. Several colleagues shared their experiences with different instruments, helping greatly in determining the pros and cons of each. These include: Terry Hemmer and Rod Buntzen of SITAC, Michael Schaepman at the University of Zurich, David Emery and Charles Kerr at the University of Southampton, Tom Lundeen of GDE Systems, Glen Franks of Innovative Imaging, Inc., and Craig Doughtry of the U. S. Department of Agriculture. Finally, the author greatly appreciates helpful reviews of the draft manuscript by Dave Beal, Tim Bowers, Tom Corl, Jim Crowley, Tom Cudahy, Jim Fry, Alex Goetz, Simon Hook, Dave Kelch, and Shelley Petroy.

7.0 REFERENCES

Berk, A., Bernstein, L. S., Robertson, D. C., 1989, MODTRAN: a moderate resolution model for LOWTRAN 7: GL-TR-89-0122, Spectral Sciences, Burlington, MA.

Buntzen, R. R., 1996, Analytical Spectral Devices FieldSpec Radiometric Calibration for Tower I: SITAC in-house report.

Fenn, R. W., Clough, S. A., Gallery, W. O., Good, R. E., Kneizys, F. X., Mill, J., Rothman, L. S., Shettle, E. P., and Volz, F. E., 1985, Optical and infrared properties of the atmosphere: Chap. 18 in *Handbook of Geophysics and the Space Environment*, Air Force Geophysics Laboratory (NTIS No. ADA 167000).

Goetz, A. F. H., Kindel, B., and Pilewaskie, P., 1998, Issues in absolute spectral radiometric calibration: Intercomparison of eight sources: Proceedings of the AVIRIS Conference, Pasadena, CA, Jan. 13, 1998.

Green, R. O., 1991, Retrieval of reflectance from AVIRIS-measured radiance using a radiative transfer code: *Proceedings of the Third Airborne Visible/Infrared Imaging Spectrometer (AVIRIS) Workshop*, JPL Publication 91-28, p. 200-210.

Green, R. O., Conel, J. E., Margolis, J. S., Buregge, C. J., and Hoover, G. L., 1991, An inversion algorithm for retrieval of atmospheric and leaf water absorption from AVIRIS radiance with compensation for atmospheric scattering: *Proceedings of the Third Airborne Visible/Infrared Imaging Spectrometer (AVIRIS) Workshop*, JPL Publication 91-28, p. 51-61.

Griffiths, P. R. and de Haseth, J. A., 1986, *Fourier Transform Infrared Spectrometry,* v. 83 in the series of monographs, *Chemical Analysis,* edited by Elving et al., John Wiley & Sons, New York.

Hemmer, Terry, 1997, Characterization of the Analytical Devices ASD FieldSpec® FR Spectrometer: SITAC in-house report.

Hook, S. and Kahle, A. B., 1996, The micro Fourier Transform interferometer (µFTIR) - a new field spectrometer for acquisition of infrared data of natural surfaces: *Remote Sensing of Environ.,* v. 56, p. 172-181.

Horton, K. A., Johnson, J. R., and Lucey, P. G., 1998, Infrared measurements of pristine and disturbed soils 2. Environmental effects and field data reduction: *Remote Sensing of Environ.*, (in press).

Hunt, G. R., Salisbury, J. W., and Lenhoff, C. J., 1971, Visible and near-infrared spectra of minerals and rocks: IV. Sulfides and sulfates: *Modern Geology*, v. 3, p. 1-14.

HYMSMO Program Office, 1997, *HYMSMO Program Ground Truth Protocol*, Spectral Information Technology Applications Center (SITAC), Fairfax, Va.

Kahle, A. B., and Alley, R. E., 1992, Separation of temperature and emissivity in remotely sensed radiance measurements: *Remote Sensing of Environment,* v. 42, p. 107-111.

Kahle, A. B., Madura, D. P., and Soha, J. M., 1980, Middle infrared multi-spectral aircraft scanner data: Analysis for geological applications: *Applied Optics*, v. 19, p. 2279-2290.

Korb, A. R. and D'Aria, 1998, Spectral emissivity and temperature retrieval, algorithms and software for infrared remote sensing data: *Remote Sensing of Environment* (submitted).

Korb, A. R., Dybwad, P. Wadsworth, W., and Salisbury, J. W., 1996, Portable Fourier transform infrared spectroradiometer for field measurements of radiance and emissivity: Applied Optics, v. 35, p. 1679-1692.

Korb, A. R., Salisbury, J. W., and D'Aria, D. M., 1998, Thermal-infrared remote sensing and Kirchhoff's Law 2: Field Measurements: *Jour. of Geophys. Res.* (in press).

Murcray, F. H., Murcray, D. G., and Williams, W. J., 1970, Infrared emissivity of lunar surface features 1. Balloon-borne observations: *Jour. of Geophys. Res.*, v. 75, p. 2662-2669.

Rowan, L. C., Bowers, T. L., Crowley, J. K., Anton-Pacheco, C., Gumiel, P., and Kingston, M. J., 1995, Analysis of airborne visible-infrared imaging spectrometer (AVIRIS) data of the Iron Hill, Colorado, carbonatite-alkalic igneous complex: *Economic Geology*, v. 90, p.1966-1982.

Salisbury, J. W., 1990, First use of a new portable thermal infrared spectrometer: Proceedings of the IEEE International Geoscience and Remote Sensing Symposium, May 20-24, 1990, College Park, MD, V. 3, p. 1775-1778.

Salisbury, J. W. and D'Aria, D. M., 1992, Emissivity of terrestrial materials in the 8-14 µm atmospheric window: *Remote Sensing of Environment*, v. 42, p. 83-106.

Salisbury, J. W. and D'Aria, D. M., 1994, Emissivity of terrestrial materials in the 3-5 µm atmospheric window: *Remote Sensing of Environment*, v. 47, p. 345-361.

Salisbury, J. W., Wald, A., and D'Aria, D. M., 1994, Thermal infrared remote sensing and Kirchhoff's Law: I Laboratory measurements: Jour. of Geophys. Res., v. 99, p.11897-11911.

Schott, J. R., 1997, *Remote Sensing: The Image Chain Approach:* Oxford University Press, NY, 394 pp.

Smith et al., 1996, Observations of infrared radiative properties of the ocean - Implications for the measurements of sea surface temperature via satellite remote sensing: *Bull. of American Meteorological Society*, v. 77, p. 41-51.

Weidner, V. R. and Hsia, J. J., 1981, Reflection properties of pressed polytetrafluoroethylene powder: Jour. Opt. Soc. Am., v. 71, p. 856-861.

APPENDIX A

GLOSSARY OF TERMS

Adjacency effect: Occurs when radiation from adjacent background materials is scattered by turbidity in the atmosphere into the line of sight of the sensor, contaminating radiance from the target.

ASD: Analytical Spectral Devices, Inc., 5335 Sterling Dr., Suite A, Boulder, CO 80301; the manufacturer of the ASD FieldSpec® FR spectrometer. Telephone (303) 444-6522, or see Web site: www.asdi.com.

ASTER: Advanced Spaceborne Thermal Emission and Reflectance Radiometer. A multispectral scanner operating in the VNIR, SWIR, and LWIR to be launched aboard the Earth Observing System EOS AM-1 satellite in 1999.

AVIRIS: The acronym variously interpreted as the "Airborne Visible/Infrared Imaging Spectrometer", and (incorrectly) as the "Advanced Visible and Infrared Imaging Spectrometer." It refers to NASA's current airborne hyperspectral imager.

Background radiance: In the reflectance region, sunlight that has been reflected from, or transmitted through, background materials (usually only significant for a specular material in reflectance, and under a tree canopy in transmittance). In the emittance region, radiation emitted by either atmospheric gases or by surrounding background materials (always significant).

Bomem: Bomem Inc., 450 ST-Jean-Baptiste Ave., Quebec, Canada G2E 5S5, the manufacturer of the Bomem MB104. Telephone (418) 877-2944 and e-mail FTIR@bomem.qc.ca.

Bidirectional reflectance: Reflectance measured at a single azimuth and angle of incidence and reflectance. This is the typical passive remote sensing measurement geometry, with the location of the sun in the sky providing the incidence azimuth and angle, and the orientation of the optical head of the sensor providing the reflectance azimuth and angle.

BRDF: Bidirectional reflectance distribution function, which describes the bidirectional reflectance values for all combinations of input and output angles. Extremes for idealized surfaces would be diffuse (Lambertian) and specular reflectance behavior.

Brightness temperature: The temperature of a blackbody with equivalent radiance to that emitted by the target at a given wavelength. If the emissivity of the target at that wavelength is less than 1.0, the true kenetic temperature is higher than the brightness temperature.

Cinnabar: HgS, the principal ore of mercury, and formerly popular as a bright red mineral pigment.

Dark current: The current that flows in a photodetector when there is no optical radiation incident on the detector. The resulting signal output must be subtracted from the signal that arises when optical radiation is incident on the detector to permit an accurate measure of radiance.

Designs and Prototypes: Designs and Prototypes, 38 Berkeley St., Nashua, NH 03060, the manufacturer of the microFTIR spectrometer. Telephone (603) 886-6736 or (860) 658-0458.

Directional hemispherical reflectance: The sample is illuminated from a given direction, and reflectance in all directions is measured, usually with an integrating sphere. This collection scheme eliminates any bias in measuring absolute reflectance due to a preferential reflectance direction.

Edge effect: Occurs when the field of view of the sensor encompasses both the ostensible target and some background material at target edge. The result is a "mixed pixel".

Emissivity: The ratio of an object's emittance to that of a blackbody at the same temperature and wavelength. Basically, this is the efficiency with which a material emits infrared radiation. When this efficiency changes with wavelength due to the presence of molecular vibration bands, an emissivity spectrum results that can often be used to determine composition.

Emittance: Flux per unit area radiated from a surface.

FTIR: "Fourier Transform Infrared." Refers to those spectrometers using interferometric techniques to measure spectral data.

GER: Geophysical and Environmental Research Corp., 1 Bennett Common, Millbrook, NY 12545, the manufacturer of the GER 3700 and Mark V spectrometers. Telephone (914)677-6100.

Halon: See Spectralon®.

HYDICE: The "hyperspectral digital imagery collection experiment," an airborne hyperspectral sensor being flown by SITAC.

HYMSMO: Hyperspectral MASINT Support to Military Operations. The HYMSMO Program is a Defense Dept. program to explore and quantify the potential utility of imaging hyperspectral sensors and data.

Hyperspectral: Tens to hundreds of bands, usually contiguous, characterized by band widths of ten nanometers or less. Usually associated with imagery obtained in each band, resulting in an image cube.

IDL: A proprietary scientific programming package.

Image cube: A stack of images, usually with hyperspectral resolution, with the x,y axes providing dimensionallity via rows of pixels, and the y dimension providing the variation of spectral reflectance for each pixel with changing wavelength.

Infrared: The region of the spectrum beyond the visible, but short of the microwave region, usually 0.75-1000 µm. The infrared is more or less arbitrarily divided into different regions, such as the NIR, SWIR, MWIR, and LWIR, defined below.

Infrared skin depth: The depth within a material over which it is emitting thermal infrared radiation. Where the absorption coefficient is high, as within molecular vibration bands, this skin depth is very small (a few tens of micrometers). Where the absorption coefficient is low, this depth may extend to hundreds of micrometers.

InGaAs: Indium gallium arsenide, a thermoelectrically-cooled detector used in the SWIR region.

InSb: Indium antinomide, a liquid nitrogen-cooled detector of the MWIR region.

Integrated Spectronics Pty. Ltd., P. O. Box 437, Baulkham Hills, NSW Australia 2153, the manufacturer of the PIMA II spectrometer. Phone: 61-2-9878-0977. FAX: 61-2-9878-3615. E-mail: ispl@intspec.com.

Irradiance: Flux per unit area onto a surface (Schott, 1997).

JPL: Jet Propulsion Laboratory, 4800 Oak Grove Dr., Pasadena, CA 91109.

Kaolinite: $Al_2Si_2O_5(OH)_4$. A clay mineral.

Kirchhoff's Law: Basically a law of reciprocity--e.g., reflectance peaks are emittance troughs and vice versa. The quantitative relationship between reflectivity and emissivity (E=1-R for opaque materials) is strictly true only under isothermal conditions, but measurements show that this relationship holds under most terrestrial environmental conditions (see Salisbury et al., 1994). Directional hemispherical reflectance must be measured to predict directional emissivity.

Labsphere, Inc.: Supplier of integrating spheres, optics, and calibration standards for wavelength, reflectance, and radiance. Located in North Sutton, NH. Telephone (603) 927-4266, or see Web site www.labsphere.com.

LWIR: Long wave infrared region of the spectrum. Usually 8-14 µm, and associated with the atmospheric window for remote sensing applications.

MASINT: Measurement and Signature Intelligence. Interpretation usually requires a computer instead of an eyeball, and includes hyperspectral remote sensing. Distinct from IMINT, Imagery Intelligence.

MCT: Mercury cadmium telluride, a liquid nitrogen-cooled detector for the LWIR region.

MIDAC: MIDAC Corp., 17911 Fitch Ave., Irvine, CA 92714, the maker of the Illuminator FTIR spectrometer.

MODTRAN: A moderate spectral resolution atmospheric model developed for the Air Force Geophysics Laboratory (Berk et al., 1989).

Multispectral: Multiple bands, usually less than ten, and not necessarily contiguous, characterized by band widths of tens of nanometers. Usually associated with imagery obtained in each band.

MWIR: Mid-wave infrared region of the spectrum. Usually 3-5 µm, and associated with the atmospheric window for remote sensing applications.

NIR: Near-infrared. Usually 0.75-1.1 µm (750-1100 nm).

NIST: National Institute of Standards and Technology. Formerly the National Bureau of Standards, NIST is a Government agency which works with industry and government to advance measurement science and develop standards (see Web site www.nist.gov).

Nyquist Frequency: The Nyquist criterion for interferometers is that the laser reference frequency must be at least twice as high as the measurement frequency for valid measurement of spectral intensity.

PbS: Lead sulfide, a detector used cooled or uncooled for measurements in the SWIR.

Planck function: The distribution of radiance with wavelength of a blackbody at a given temperature.

Pyrophyllite: $Al_2Si_4O_{10}(OH)_2$. A mica.

Radiance: Flux per unit projected area per unit solid angle from, onto, or through a surface (Schott, 1997).

Realgar: AsS, formerly used as an orange mineral pigment.

Reststrahlen bands: The fundamental molecular vibration bands of solids, which are reflectance peaks and emittance troughs. Polished minerals were used as crude reflectance filters in early optical research, because of their strong reflectance at wavelengths associated with their fundamental molecular vibration bands, which vary in wavelength from mineral to mineral. This is the origin of the term "reststrahlen bands" from the German for "residual rays."

SITAC: Spectral Information Technology Applications Center, 11781 Lee Jackson Memorial Highway, Suite 500, Fairfax, VA 22033. Telephone 703-591-8546.

Skylight: Direct sunlight scattered by atmospheric molecules and/or aerosols.

Spectral International: U. S. Distributor of the PIMA II active spectrometer. Address: P. O. Box 1027, Arvada, CO 80001. Telephone number: 303-403-8383. FAX: 303-403-8385. E-mail: mail@pimausa.com. (For Canadian sales, PetraScience Consultants, 3995 W. 24th Ave., Vancouver, BC. Telephone/fax number: 604-222-4642. E-mail: petrascience@compuserve.com.)

Spectralon®: Proprietary reflectance standard material sold by Labsphere, Inc. of North Sutton, NH. It is composed of sintered Halon, which is the trade name for polytetrafluoroethylene powder (Weidner and Hsia, 1981). In its pure form, it is more than 99% reflecting in the VNIR, but its reflectance declines slightly in the UV and SWIR (see Section 5.2.1).

Stibnite: Sb_2S_3, the chief ore mineral of antimony.

SWIR: Short wave infrared region of the spectrum. Usually 1.1-2.5 µm (1100-2500 nm).

TIR: Thermal infrared, meaning that portion of the spectrum where the remotely sensed radiation is dominated by self-emission of surface materials, rather than reflected sunlight. This includes both the MWIR and LWIR.

UV: Ultraviolet region of the spectrum. Usually 1.0-400 nm.

VNIR: Visible and near-infrared regions of the spectrum. Usually 0.4-1.1 µm (400-1100 nm).

Visible: The region of the spectrum to which the human eye is sensitive. Usually 0.4-0.75 µm (400-750 nm).

Zenith angle: The angle of the sun with respect to the vertical. Thus, a large zenith angle is close to the horizon. A source of confusion is solar elevation angle, which is the angle of the sun with respect to the horizon.

Ward's Natural Science Establishment: Supplier of mineral and other natural science materials in Rochester, NY. Telephone 1-800-962-2660, or see Web site www.wardsci.com.